Defence Research and Development Canada
Recherche et développement pour la défense Canada

DEFENCE R&D DÉFENSE

Multidisciplinary integrated analysis for engagement simulation of hypersonic weapons

Richard Lestage
François Lesage
Robert A. Stowe
Nicolas Hamel
DRDC Valcartier

Defence R&D Canada – Valcartier
Technical Memorandum
DRDC Valcartier TM 2010-085
May 2010

Canada

Multidisciplinary integrated analysis for engagement simulation of hypersonic weapons

Richard Lestage
François Lesage
Robert A. Stowe
Nicolas Hamel
DRDC Valcartier

Defence R&D Canada – Valcartier

Technical Memorandum
DRDC Valcartier TM 2010-085
May 2010

Principal Author

Richard Lestage

Defence Scientist

Approved by

Alexandre Jouan

Section Head, Precision Weapons Section

Approved for release by

Christian Carrier

Chief Scientist

This work has been performed from April 2005 to March 2007 under project 13eu04, "Capability engineering for hypersonic airbreathing weapons"

Abstract

The emergence of missiles flying in the hypersonic regime brings a new series of technical challenges such as, strong system integration of aerodynamics, propulsion and structures, and problems with thermal management. To address these challenges, a multidisciplinary integrated analysis tool which permits to perform a complete engagement simulation using a six-degree-of-freedom flight mechanics models was developed. The tool is used to perform parametric study for missile sizing, performance trade-off and optimization. Additionally, it assesses the effect of vehicle design variables on the flight time, the trajectory and the velocity profile. A baseline missile reference was established as a starting point on which the impact of various design variables is assessed. The various sensitivity and trade-off analyses performed on key missile design variables allowed observing several interesting interactions and learning key lessons to apply to the design and analysis of hypersonic missiles. To demonstrate the application of optimization techniques to the design of hypersonic missiles, a simple time of flight optimization problem is presented. The multidisciplinary integrated analysis tool presents basic analysis capabilities for all subsystems critical to the study of hypersonic weapon systems. However, most subsystem models are limited in fidelity and details and would benefit from improvements. The most significant deficiencies are the lack of an airbreathing propulsion model and the non support of non-symmetric airframe configurations such as wave-riders. The support of wave-rider type configurations would require significant changes to most subsystems models.

Résumé

L'émergence de missiles battant dans le régime hypersonique apporte une nouvelle série de défis technologiques tels qu'un niveau élevé d'intégration de l'aérodynamique, de la propulsion et des structures ainsi que des problèmes avec la gestion thermique. Pour relever ces défis, un outil d'analyse intégrée pluridisciplinaire qui permet d'effectuer une simulation complète d'engagement à l'aide d'un modèle de mécanique du vol à six degrés de liberté a été développé. L'outil est utilisé pour effectuer des études paramétriques pour le dimensionnement des missiles, l'étude des compromis de performances et l'optimisation. En outre, il évalue l'effet des paramètres de conception du véhicule sur le temps de vol, la trajectoire et la vitesse de vol. Un modèle de missile de référence a été établi comme point de départ sur lequel est évalué l'impact des différents paramètres de conception. Les analyses de sensibilité et les études effectuées sur les paramètres de conception de missiles ont permis l'observation de plusieurs interactions intéressantes ainsi que l'apprentissage des leçons clés à appliquer à la conception et à l'analyse des missiles hypersoniques. Pour démontrer l'application des techniques d'optimisation à la conception de missiles hypersoniques, un problème simple d'optimisation de temps de vol est présenté ici. L'outil d'analyse intégrée pluridisciplinaire présente des capacités d'analyse de base pour tous les sous-systèmes critiques pour l'étude des systèmes d'armes hypersoniques. Toutefois, la plupart des modèles de sous-systèmes sont limités au niveau de la fidélité et des détails et bénéficieraient d'améliorations. Les déficiences les plus importantes sont l'absence d'un modèle de propulsion aérobie et l'absence de prise en charge de configurations non symétriques comme les "wave-rider". La prise en charge de configurations de type "wave-rider" nécessiterait des changements significatifs pour la plupart des modèles de sous-systèmes.

This page intentionally left blank.

Executive summary

Multidisciplinary integrated analysis for engagement simulation of hypersonic weapons:

Richard Lestage; François Lesage; Robert A. Stowe; Nicolas Hamel; DRDC Valcartier TM 2010-085; Defence R&D Canada – Valcartier; May 2010.

The emergence of missiles flying in the hypersonic regime brings a new series of technical challenges such as, strong system integration of aerodynamics, propulsion and structures, and problems with thermal management. To address these challenges, a multidisciplinary integrated analysis tool which permits to perform a complete engagement simulation using a six-degrees-of-freedom flight mechanics models was developped. The tool presented in this document integrates the following subsystem models: External Geometry Definition, aerodynamic prediction, internal components definition, solid rocket motor, airframe physical characteristic, autopilot tuning, trajectory simulation, aerodynamic heating, structure heat transfer and conduction.

The tool is used to perform parametric studies for missile sizing, performance trade-off and optimization. Additionally, it assesses the effect of vehicle design variables on the flight time, the trajectory and the velocity profile. Measures of vehicle integrity such as aerodynamic stability, controllability and thermal analysis are included to ensure that the hypersonic missile studied is conceptually sound.

A baseline missile reference was established as a starting point on which the impact of various design variables is assessed. The various sensitivity and trade-off analyses performed on key missile design variable allowed observing several interesting interactions and learning key lessons to apply to the design and analysis of hypersonic missiles.

To demonstrate the application of optimization techniques to the design of hypersonic missiles, a simple time of flight optimization problem is presented. The time of flight was significantly reduced by adjusting the propulsion sustain phase duration to match the flight time. Missile dimensions and mass differences between the baseline and the optimum are not large.

The multidisciplinary integrated analysis tool presents basic analysis capabilities for all subsystems critical to the study of hypersonic weapon systems. However, most subsystem models are limited in fidelity and details and would benefit from improvements. The most significant deficiencies are the lack of an airbreathing propulsion model and the non support of non-symmetric airframe configurations such as wave-riders. The support of wave-rider type configuration would require significant changes to most subsystem models.

Sommaire

Multidisciplinary integrated analysis for engagement simulation of hypersonic weapons:

Richard Lestage; François Lesage; Robert A. Stowe; Nicolas Hamel; DRDC Valcartier TM 2010-085; R & D pour la défense Canada – Valcartier; Mai 2010.

L'émergence de missiles battant dans le régime hypersonique apporte une nouvelle série de défis technologiques tels qu'un niveau élevé d'intégration de l'aérodynamique, de la propulsion et des structures ainsi que des problèmes avec la gestion thermique. Pour relever ces défis, un outil d'analyse intégrée pluridisciplinaire qui permet d'effectuer une simulation complète d'engagement à l'aide d'un modèle de mécanique du vol à six degrés de liberté a été développé. L'outil présenté dans ce document intègre les sous-systèmes des modèles suivants : définition de géométrie externe, prédiction aérodynamique, définition des composants internes, moteur-fusée à carburant solide, caractéristique physique de la cellule, réglage du pilote automatique, simulation de trajectoire, échauffement aérodynamique, transfert de chaleur et conduction.

L'outil est utilisé pour effectuer des études paramétriques pour le dimensionnement des missiles, l'étude des compromis de performances et l'optimisation. En outre, il évalue l'effet des paramètres de conception du véhicule sur le temps de vol, la trajectoire et la vitesse de vol. Des mesures de l'intégrité du véhicule telle que la stabilité aérodynamique, la contrôlabilité et l'analyse thermique sont inclus pour garantir que le missile hypersonique étudié est viable du point de vue conceptuel.

Un modèle de missile de référence a été établi comme point de départ sur lequel est évalué l'impact des différents paramètres de conception. Les analyses de sensibilité et les études effectuées sur les paramètres de conception de missiles ont permis l'observation de plusieurs interactions intéressantes ainsi que l'apprentissage des leçons clés à appliquer à la conception et à l'analyse des missiles hypersoniques.

Pour démontrer l'application des techniques d'optimisation à la conception de missiles hypersoniques, un problème simple d'optimisation de temps de vol est présenté ici. Le temps de vol a été considérablement réduit en ajustant la propulsion afin que la durée de la poussée corresponde au temps de vol. Les dimensions et la masse du missile optimisé diffèrent peu du modèle de référence.

L'outil d'analyse intégrée pluridisciplinaire présente des capacités d'analyse de base pour tous les sous-systèmes critiques pour l'étude des systèmes d'armes hypersoniques. Toutefois, la plupart des modèles de sous-systèmes sont limités sur le plan de la fidélité et des détails et bénéficieraient d'améliorations. Les déficiences les plus importantes sont l'absence d'un modèle de propulsion aérobie et l'absence de prise en charge de configurations non symétriques comme les "wave-rider". La prise en charge de configurations de type "wave-rider" nécessiterait des changements significatifs pour la plupart des modèles de sous-systèmes.

Table of contents

List of figures

List of tables

This page intentionally left blank.

1 Introduction

Under projects 13eu (CEFHAW "Capability engineering for hypersonic airbreathing weapons") and 13na (IHPS "Integrated hypersonic technologies for long-range precision strike"), DRDC Valcartier has initiated the development, demonstration and validation of a capability to evaluate enabling technologies of hypersonic airbreathing missiles. These projects have led to the development of an expertise in the fundamental physical processes for hypersonic flight, through modelling and experiments, and to the creation of a basic version of a performance prediction tool for the flight of a hypersonic airbreathing missile.

This Technical Memorandum presents a multidisciplinary integrated analysis tool to assess the performance of hypersonic missiles and shows typical results.

The development of tools and capabilities for missiles flying in the hypersonic regime brings a new series of challenges. Kors [1] and Naidu et al. [2] provide a good overview of the history hypersonic technology and identify key challenges. The following three problematic below are retained.

a. Strong system integration of aerodynamics, propulsion and structures

   Because the airframe geometry of a hypersonic airbreathing missile is strongly affected by the propulsion inlet and nozzle, the structure and the aerodynamic are also strongly affected [1][2]. The aerodynamics, propulsion and structure designs need to be integrated. The aeroelasticity is also more complex because geometry changes directly affect the propulsion performance [3].

b. Propulsion needing to perform over a wide operating range of conditions

   Since propulsion is sensitive to angle of attack and dynamic pressure, trajectory shaping becomes an important factor [1][2]. It is thus important to consider off-design performance of propulsion during transient flight periods. Also, trajectory and flight-engine control strategies must be carefully selected to optimize engine operation [3].

c. High temperature needing thermal management

   Because of high speed and high dynamic pressure, aerodynamic induced heating is significant on hypersonic missiles [1][2]. In addition to aerodynamic properties consideration, the design of missile stagnation point location such as leading edge and control surfaces must consider aerodynamic heating and temperature elevation to ensure that structure integrity is maintained.

To achieve the engineering capability to perform analysis of hypersonic airbreathing weapons, a multidisciplinary integrated analysis tool needs to be developed to study the problematic and the challenges identified. Additionally, performance prediction shall be performed in term of system kinematic mission performance (time-velocity-space from launch to target) rather than subsystem performances.

To address the aerodynamics, propulsion and structures integration, several authors performed the analysis using mass-drag-propulsion optimization on cruising trim condition [4-11]. While this approach permits to study aerodynamics, propulsion and structures integration, it does not capture the effect of off-design operation at angle-of-attack and non-optimal dynamic pressure.

Some analysis work includes complex trajectory simulation with off-design propulsion analysis [12] but do not permit parametric studies on missile design variables. Very few include impact of aerodynamic heating and thermal management [13][14][15].

The analysis tool developed at DRDC permits to perform a complete engagement simulation using a six-degree-of-freedom flight mechanics model. Although using limited fidelity subsystem models, the tool allows performing parametric study for sizing, trade-off and optimization. Additionally, it is able to assess the effect of vehicle design variables on the flight time, trajectory and velocity profile. Some measures of vehicle integrity such as aerodynamic stability, controllability and thermal analysis are included to ensure that the hypersonic missile studied is conceptually sound.

The structure of the system performance tool will be presented in Chapter 2 and, the various subsystem models, in Chapter 3. The capability for design trade-off and sensitivity analyses will be presented in Chapter 4 and, the optimization capability, in Chapter 5.

2 System performance modelling and analysis tool

Missile system design requires high levels of integration among disciplines such as aerodynamics, structures, propulsion, and controls.

These disciplines are interactive and coupled and these effects must be fully considered in the analysis of missiles and in the prediction of system responses.

The system performance model and the analysis must therefore consider the interaction between disciplines and technologies. To address these issues, several subsystem models have been integrated into a simulation environment that allows the required interactions to be studied. The proposed solution is similar to other approaches [14][15][16].

The visual environment for process integration ModelCenter^{tm}[17], from Phoenix Integration Inc., has been used to integrate the following subsystem models:

- External Geometry Definition ;
- Missile Datcom Aerodynamic Prediction ;
- Internal Missile Components Definition ;
- Solid Rocket Motor Propulsion;
- Airframe Physical Properties ;
- Autopilot Tuning ;
- Aerodynamic Stability Margin
- Structure First Mode Bending Frequency
- Trajectory Computation ;
- Aerodynamic Heating ; and
- Conduction and Structure Temperature.

Model names above are capitalized in this document to emphasis reference to a specific subsystem model rather than a literal expression.

ModelCenter uses wrapping functions and plug-ins to interface the subsystem model in the ModelCenter environment. Using a link editor, output from subsystem models can be connected to input of other subsystems to allow subsystem model to interact together.

The interaction between individual subsystems is graphically illustrated in Figure 1.

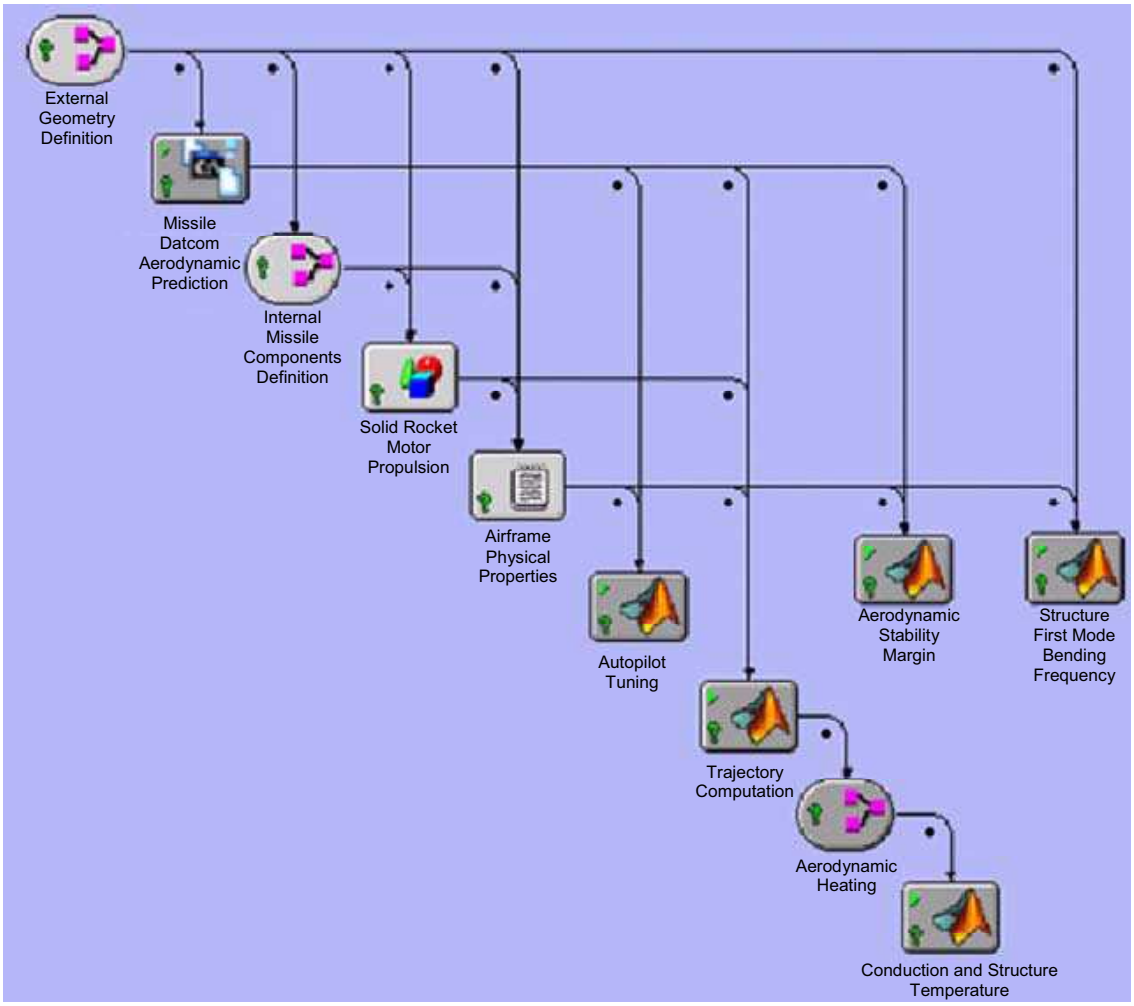

Figure 1: Integration of subsystem models in Phoenix Integration's ModelCenter [17].

3 Subsystems models

This section presents an overview of each of the subsystem model used in the system performance tool.

3.1 External Geometry Definition

The External Geometry Definition of the missile describes the external shape of the missile.

It is an assembly composed of a structure and fins. The variable properties of the external geometry are listed in Table 1. An example of geometry is illustrated in Figure 2.

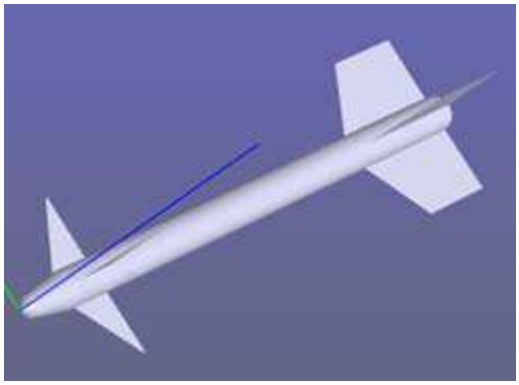

Figure 2: Example of external geometry.

This subsystem model outputs the description of the geometry in a string format suitable for processing by Missile DATCOM [19].

Table 1: Variables of the External Geometry Definition.

Variable	Units	Description
Inputs:		
AxisymmetricBody1.LNOSE	m	Nose length
AxisymmetricBody1.DNOSE	m	Nose diameter
AxisymmetricBody1.BNOSE	m	Nose bluntness radius
AxisymmetricBody1.LCENTR	m	Body length
AxisymmetricBody1.DCENTR	m	Body diameter
AxisymmetricBody1.BodyThickness	m	Body thickness
AxisymmetricBody1.BodyMaterialDensity	kg/m^3	Body material density
FinSet1.SSPAN1	m	Fin span from center line to base
FinSet1.SSPAN2	m	Fin span from center line to tip
FinSet1.CHORD1	m	Fin chord length at base
FinSet1.CHORD2	m	Fin chord length at tip

FinSet1.SWEEP	deg	Fin sweep angle
FinSet1.XLE	m	Fin trailing edge distance from nose
FinSet1.FinThickness	m	Fin thickness
FinSet1.FinMaterialDensity	kg/m^3	Fin material density
FinSet2.SSPAN1	m	Fin span from center line to base
FinSet2.SSPAN2	m	Fin span from center line to tip
FinSet2.CHORD1	m	Fin chord length at base
FinSet2.CHORD2	m	Fin chord length at tip
FinSet2.SWEEP	deg	Fin sweep angle
FinSet2.XLE	m	Fin trailing edge distance from nose
FinSet2.FinThickness	m	Fin thickness
FinSet2.FinMaterialDensity	kg/m^3	Fin material density
Outputs:		
LengthMissile	m	Length of missile
DatcomBodyStr	-	String of text describing the geometry in the Missile DATCOM format
Geometry	-	Data structure that comprises geometrical and mass properties of the external geometry (Defined as per Table 2)

The Geometry output variable is a structure of data that provides inform about mass, moments of inertia, orientation and location of center of gravity (CG). Variables of Geometry data structure are shown in Table 2. Mass properties are estimated using uniform thin cylinder approximation for the missile structure and uniform thin plates for the fins [18]. These mass properties are used as input to the Airframe physical properties subsystem model.

Table 2: Properties of the Geometry data structure.

Variable	**Units**	**Description**
Orientation.Rotate_X	rad	Rotation of the geometry wrt X reference axis
Orientation.Rotate_Y	rad	Rotation of the geometry wrt Y reference axis
Orientation.Rotate_Z	rad	Rotation of the geometry wrt Z reference axis
Orientation.Translate_X	m	Translation of the geometry wrt X reference axis
Orientation.Translate_Y	m	Translation of the geometry wrt Y reference axis
Orientation.Translate_Z	m	Translation of the geometry wrt Z reference axis
MassProperties.CG_X	m	CG X location wrt missile nose
MassProperties.CG_Y	m	CG Y location wrt missile nose
MassProperties.CG_Z	m	CG Z location wrt missile nose
MassProperties.Volume	m^3	Volume
MassProperties.SurfaceArea	m^2	Surface Area
MassProperties.Mass	kg	Mass
MassProperties.Ixx	$kg.m^2$	X axis polar moment of inertia wrt CG
MassProperties.Iyy	$kg.m^2$	Y axis polar moment of inertia wrt CG

MassProperties.Izz	kg.m²	Z axis polar moment of inertia wrt CG
MassProperties.IsConsumable	Boolean	Flag identifying consumable material (e.g. propellant)

3.2 Missile Datcom Aerodynamic Prediction

The Missile Datcom Aerodynamic Prediction subsystem builds a database of aerodynamic coefficients based on the geometry defined by the External Geometry Definition subsystem.

The database is a multi-dimensional look-up table for the aerodynamic coefficients of Table 3.

Table 3: Aerodynamic coefficients database.

Coefficient	**Definition**
C_a	Axial force coefficient
C_{ll}	Roll moment coefficient
C_{llp}	Roll damping moment coefficient
C_{ln}	Yaw moment coefficient
C_{lnr}	Yaw damping moment coefficient
C_m	Pitch moment coefficient
$C_{mâ}$	Downwash moment coefficient
C_{mq}	Pitch damping coefficient
C_N	Normal force coefficient
C_Y	Normal damping coefficient
d_{ref}	Reference diameter for surface and moment (m)
x_{ref}	Longitudinal reference position for moment (m from missile nose)

The multi-dimensional look-up table for each coefficient is 7 dimensions to allow to interpolate as function of:

- Mach number (M)
- Total aerodynamic angle of attack (α_T)
- Roll angle of the angle of attack with respect to missile body (ϕ_T)
- Control deflection angle of fin 1 (δ_1)
- Control deflection angle of fin 2 (δ_2)
- Control deflection angle of fin 3 (δ_3)
- Control deflection angle of fin 4 (δ_4)

Coefficients are computed using the Missile Datcom [19] aerodynamic software prediction tool.

3.3 Internal Missile Component Definition

The Internal Missile Component Definition subsystem allows taking into consideration the volume and mass of internal components such as the seeker, the guidance navigation and control (GNC) and the warhead as illustrated in Figure 3.

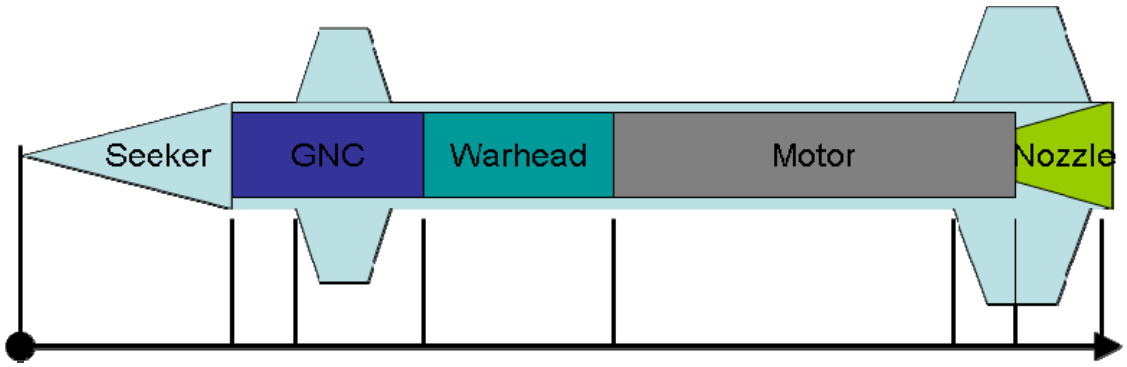

Figure 3: Layout of missile internal components.

It assumes a cylinder of uniform density for each internal component. Each component is defined by the variables of Table 4

Table 4: Variables of Internal Missile Component Definition.

Variable	Units	Description
Inputs:		
Diameter	m	Diameter
XLEFront	m	Component front end location measured from missile nose
Length	m	Length of component
MaterialDensity	kg/m^3	Component material density
Outputs:		
XLEEnd	m	Component rear end location measured from missile nose. Used to locate front end of next component.
Geometry	-	Data structure that comprise geometrical and mass properties of the internal component (Defined as per Table 2) used as input to the “Airframe Physical Properties” subsystem model.

3.4 Solid Rocket Motor Propulsion

A missile rocket motor total impulse is dictated by the size of the motor. This total impulse is then distributed over time during the boost and the sustain propulsion phase. The boost phase is of short duration and provides the missile with its initial velocity. The sustain thrust is then used to

maintain initial velocity until all propellant is consumed. The Solid Rocket Motor Propulsion model subsystem computes a rocket motor thrust curve given a desired thrust and the available volume of propellant. This subsystem allows the missile designer to specify the fraction of the total motor impulse to use for the boost phase and allows using the remaining impulse to sustain the missile flight.

The total motor impulse is first estimated using the volume of propellant contained in the specified motor dimensions. If the total motor impulse is greater than the desired boost impulse, a "boost-sustain" thrust profile is computed where the sustain thrust is maintained until total impulse is consumed (Figure 4).

If the total motor impulse is less than the desired boost impulse, a "boost-only" thrust profile is computed where the impulse is consumed during at boost thrust (Figure 5).

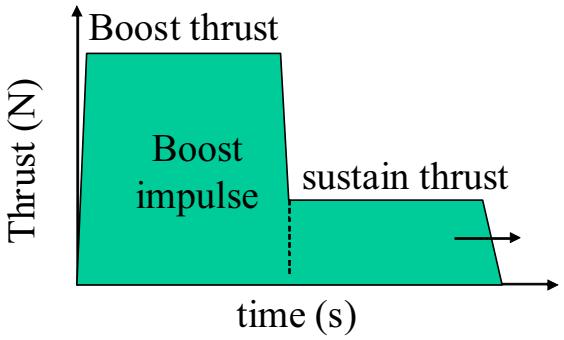

Figure 4: Boost-sustain thrust profile. Duration of sustain phase depends on available total motor impulse.

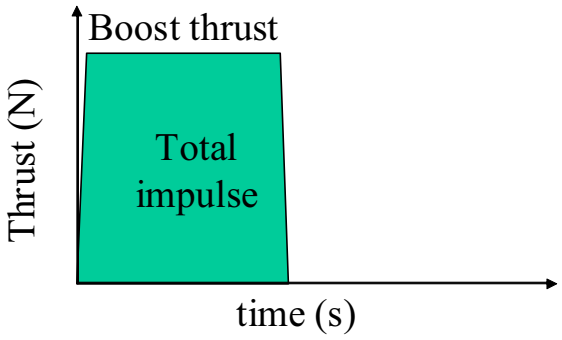

Figure 5: Boost thrust profile. Duration of boost phase depends on available total motor impulse.

The independent input variables and computed outputs of the propulsion model are presented in Table 5.

Table 5: Variables of the Solid Rocket Motor Propulsion model.

Variable	**Units**	**Description**
Inputs:		
MotorLength	m	Motor length
BoostThrust	N	Motor thrust during boost phase
DesiredSustainThrust	N	Motor thrust during sustain phase
DesiredBoostImpulse	N.s	Desired Boost phase impulse
XLEfront	m	Motor front end distance from nose
Diameter	m	Motor diameter
PropellantDensity	kg/m^3	Propellant density
PropellantIsp	s	Propellant specific impulse
PropellantVolumeFraction		Propellant volume fraction
SustainThrust	N	Motor thrust during sustain phase

Outputs:		
XLEend	m	Motor rear end distance from nose
TotalImpulse	Ns	Total impulse of motor
NozzleExitArea	m²	Motor nozzle exit area
MotorThrustVector	N	Vectors of thrust as a function of mass obtained by the combustion of the solid rocket motor
MotorMassVector	kg	Vectors of mass used for thrust
Geometry	-	Data structure that comprise geometrical and mass properties of the internal component (Defined as per Table 2) used as input to the "Airframe Physical Properties" subsystem model.

3.5 Airframe Physical Properties

The Airframe Physical Properties of the complete missile airframe are computed by adding the contributions of the subsystems geometries (External Geometry Definition (body and fins), Internal Missile Component Definition (seeker, guidance, actuator and warhead) and Solid Rocket Motor Propulsion). Values are computed for launch and burn-out states. At burn-out state, the geometries that are defined as consumable have no contribution.

3.6 Autopilot Tuning

The Autopilot Tuning subsystem performs the design of a lateral acceleration autopilot for the physical and aerodynamic properties of the missile.

It first builds a linear plant model of the airframe and then selects autopilot gains to achieve the given closed-loop specification:

$$\frac{a(s)}{a_{cmd}(s)} = \frac{\left(As^2 + Bs + C\right)}{\left(s + \mu\right)\left(s^2 + 2z\omega s + \omega^2\right)} \qquad \text{(eq. 1)}$$

It uses 4 fins where the lateral fins can be actuated differentially to provide roll control. The gains are stored in a table for each combination of Mach and altitude. More details on the method used can be found in reference [20].

3.7 Aerodynamic Stability Margin

The aerodynamic stability is an important factor in the design of a missile. Stability margin is function of the aerodynamic center of pressure that varies with Mach number and function of center of gravity location which depends on the amount of remaining combustible in the missile. The Aerodynamic Stability Margin subsystem computes the worst case static stability margin for all Mach numbers and with the worst center of gravity location.

The aerodynamic stability margin is expressed in calibre and is the distance between the aerodynamic center of pressure and the center of gravity.

A positive stability margin indicates stability. More stability usually requires larger aerodynamic surfaces that create drag. Less stability usually creates control stability problems. A common rule of thumb for missile design is to aim for a stability margin of one calibre.

3.8 Structure First Mode Bending Frequency

Missile structure stiffness is important to prevent flutter or aeroservoelastic instability. The missile Structure First Mode Bending Frequency is a good indication of the structural integrity of a missile.

The airframe is approximated as a tube of uniform mass distribution to compute the first mode bending frequency ω:

$$\omega = 22.373\sqrt{\frac{\varepsilon I}{\rho L_{missile}^{\ 4}}} \qquad \text{(eq. 2)}$$

where :

- ε is the Young's modulus of elasticity of the missile structural tube;
- $I = \pi d^3 t/8$ is the area moment inertia of the missile structural tube of thickness t and diameter d;
- $\rho = m_{missile}/L_{missile}$ is the mass per unit length of the missile.

A rule of thumb for missile design is to aim for a structure first mode bending frequency superior to twice the natural aerodynamic pitching frequency and twice the autopilot bandwidth frequency.

3.9 Trajectory Computation

Having defined missile geometry, aerodynamic coefficient, mass, propulsion and autopilot, an engagement simulation can be computed to evaluate missile performance such as time of flight, velocity, range and flight profile. The six-degree-of-freedom (6DOF) simulation model has been implemented in Matlab/Simulink using MSTARSDRDC Toolbox. MSTARSDRDC is a collection of Simulink library blocks that allows the simulation of weapons. The model guidance has been configured to follow trajectory defined by waypoints. Figure 6 illustrates the top view of the model.

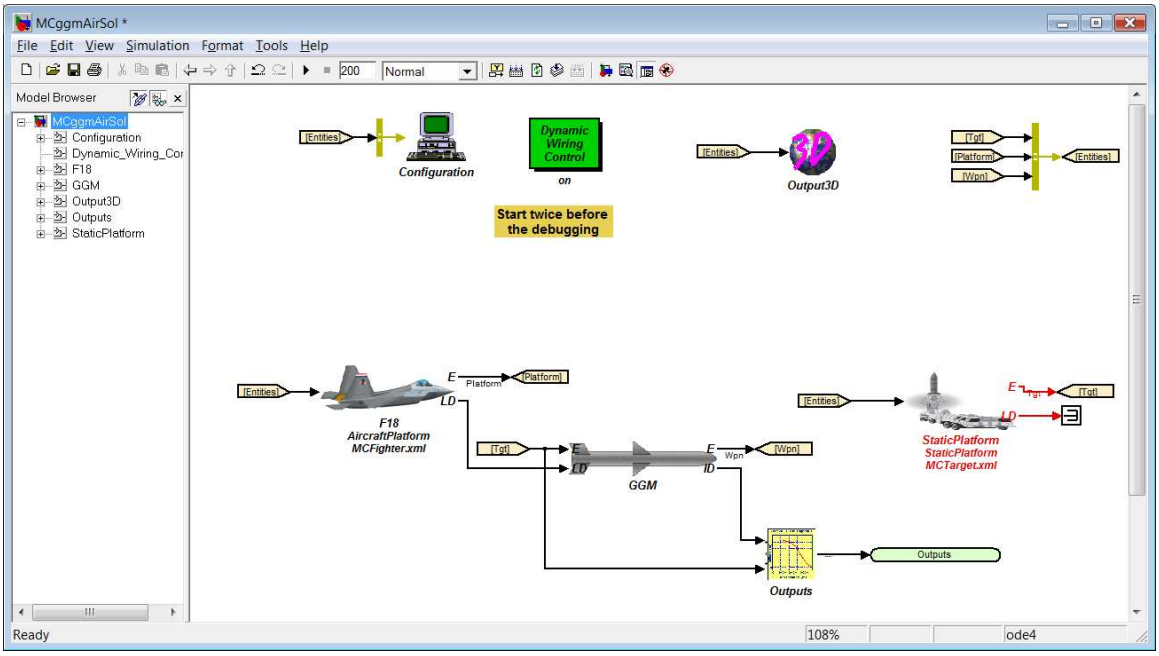

Figure 6: MSTARSDRDC 6DOF Simulink Model.

3.10 Aerodynamic Heating

During hypersonic flight, aerodynamic heat becomes an important factor to be considered. Control surface leading edges and missile nose are subject to high temperatures that can create serious material degradation.

The Aerodynamic Heating subsystem model computes the heating flux at a series of positions (typically 25) equally spaced on the missile surface. The heat flux computation is performed for a given missile surface temperature and for a series of position and velocity following the missile trajectory.

Computation uses the U.S. Army Ballistic Research Laboratory Interact [21][22] aeroheating prediction software. Interact is limited to blunt cone-cylinder-flare projectiles as illustrated in Figure 7.

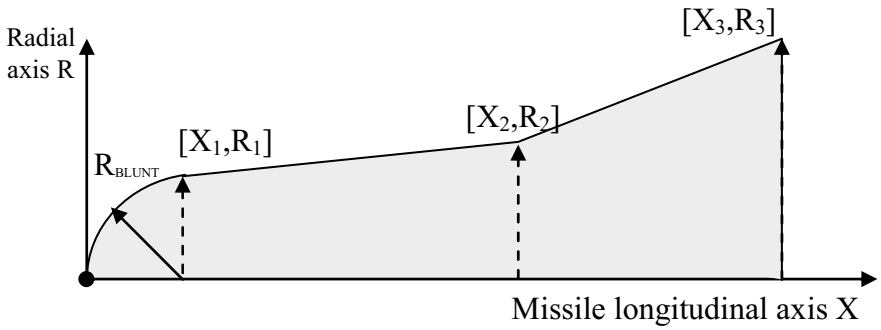

Figure 7: Blunt cone-cylinder-flare projectile geometry used for "Interact".

Because the geometry used for aerodynamic heating computation differs from the "External Geometry Definition (section 3.1), the Aerodynamic Heating model was used only to compute the heat transfer on the missile nose since it cannot appropriately represent the canards and back-end of the complete missile geometry.

3.11 Conduction and Structure Temperature

To assess the effect of aerodynamic heat on missile structure temperature, a Conduction and Structure Temperature code has been implemented to compute the dynamic temperature variation.

A solid axi-symmetric uniform geometry similar to the Interact geometry has been decomposed in a grid of 5x20 cells (Figure 8).

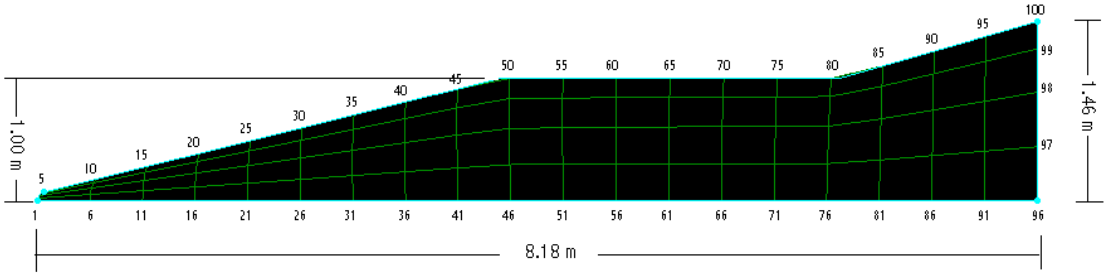

Figure 8: Conduction Geometry.

Graphical illustration of temperature distribution inside missile geometry at a given time during flight is presented in Figure 9.

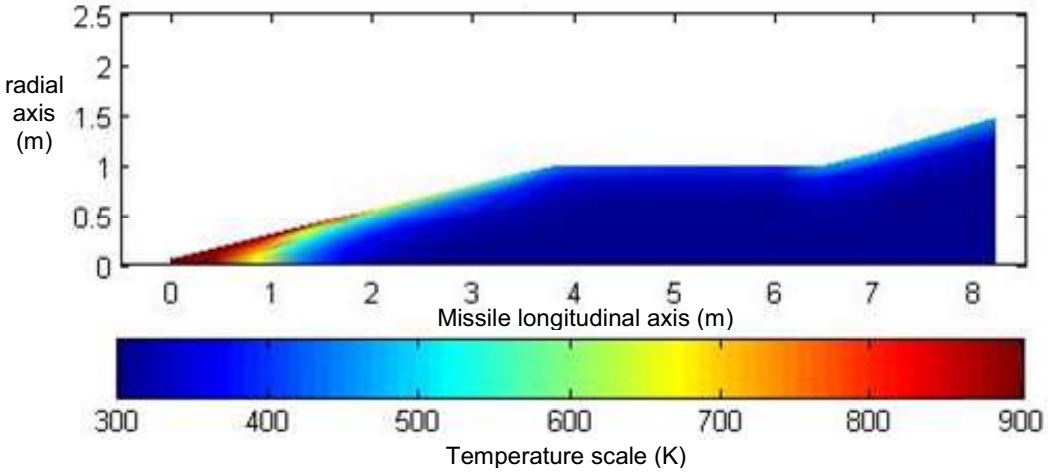

Figure 9: Temperature distribution inside missile geometry.

Several numerical limitations have been observed in the conduction code. The number of cells in the geometry is not large enough and skewness of cells has not been properly taken into account for cell-to-cell conduction.

Because of these limitations, it is recommended that future work on hypersonic missile system performance studies use SHEMAC[23][24] instead of the conduction code used here.

4 Design trade-off and sensitivity analysis

The missile system performance tool allows performing design and trade-off studies of missile system. This section presents results for different types of studies. First, a baseline reference is established as a starting point on which the impact of various design variables is assessed.

4.1 Baseline design

The number of possible missiles configuration being unlimited, a baseline air-to-surface missile design is established.

Table 6 presents the variables of the baseline design and their initial values. In order to limit the number of variables of the concept, the geometry is entirely defined by the missile diameter, the missile length and the fin span as shown on Figure 10. The resulting configuration is illustrated in Figure 11.

Table 6: Variables of baseline design

Variables	Baseline value
Diameter ϕ (m)	0.175
Missile length $L_{missile}$ (m)	6.5
Fin span d (m)	0.35
Boost thrust (N)	35 000
Boost impulse (N.s)	160 000
Sustain thrust (N)	4000
Skin material thickness (m)	0.005
Nose radius (m)	0.04
Cruise altitude (m)	10 000

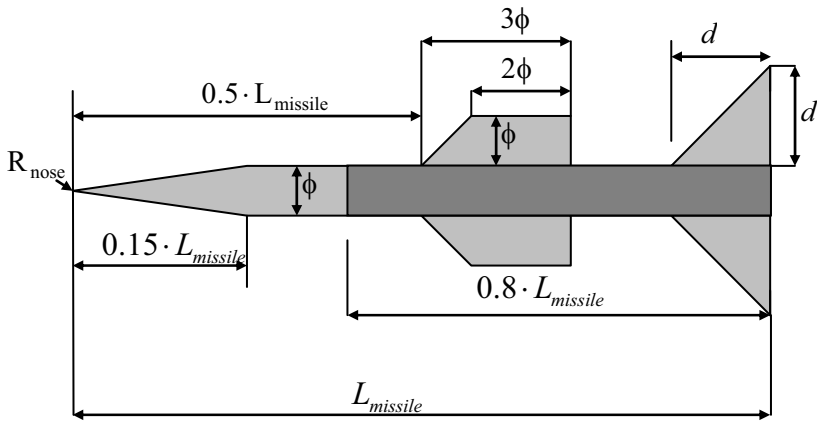

Figure 10: Coupling relationship for the baseline geometry

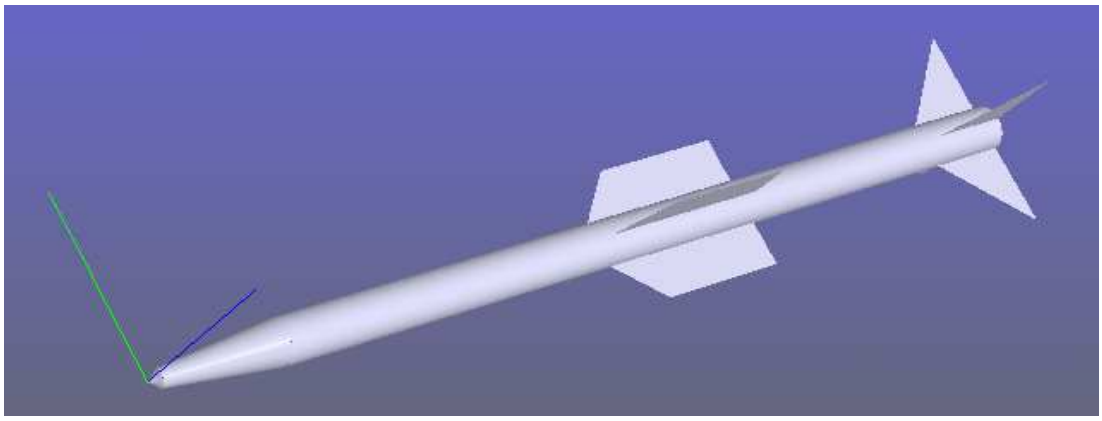

Figure 11: Illustration of baseline geometry

Table 7 presents some of the critical missile properties and performance factors obtained for the baseline missile for a 100 km range air-to-surface engagement. An exhaustive list of all variables and results for this configuration is presented in Annex A.

Table 7: Baseline critical missile properties and performance factors

Variables	Values
Stability margin (ϕ)	0.806
Missile mass (kg)	299.2
First mode bending frequency (rad/s)	66.99
Time of flight (s)	100.52
Final nose temperature (K)	2171.3

The resulting trajectory altitude and Mach number are plotted as a function of range in Figure 12. Figure 13 presents the same results plotted as a function of time.

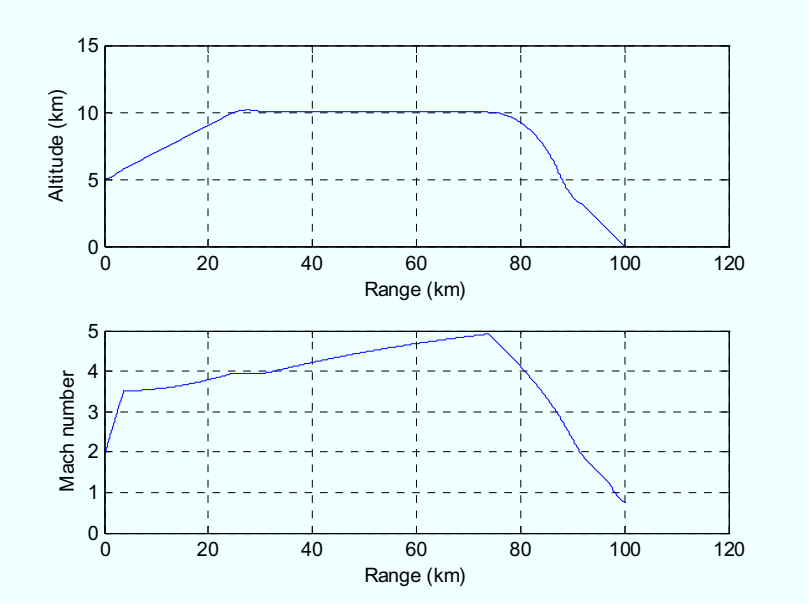

Figure 12: Baseline missile altitude and velocity as a function of range.

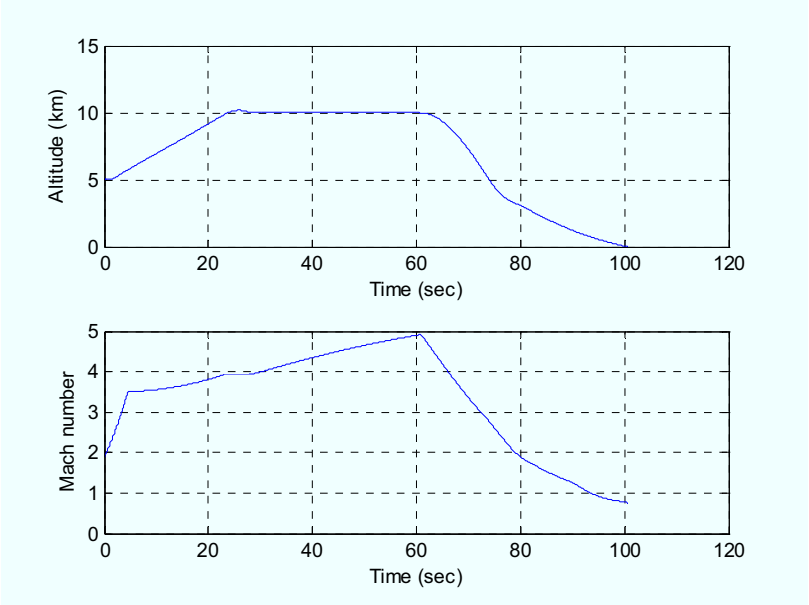

Figure 13: Baseline missile altitude and velocity as a function of time.

During high-speed flight, the missile nose is subject to aerodynamic heating. Figure 14 presents the heat transfer flux at the nose of the missile during the entire flight. Heating peaks at highest velocity even if it coincides with lowest air density (highest altitude). When the missile dives toward the surface target, velocity and heating start decreasing but nose temperature continues to increase until velocity decreases below Mach 1.5. Figure 14 also shows the evolution of the nose temperature. The resulting temperature distribution is shown in Figure 15.

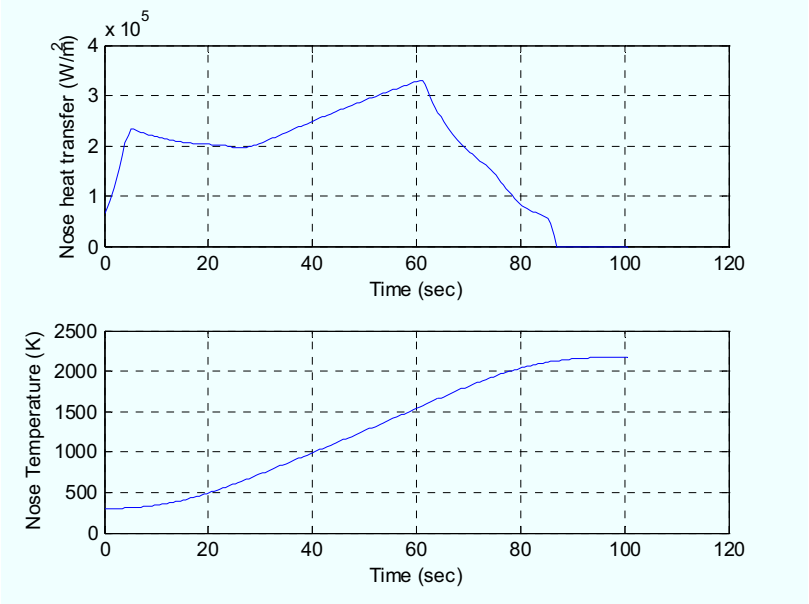

Figure 14: Baseline missile nose heat transfer and temperature evolution during flight.

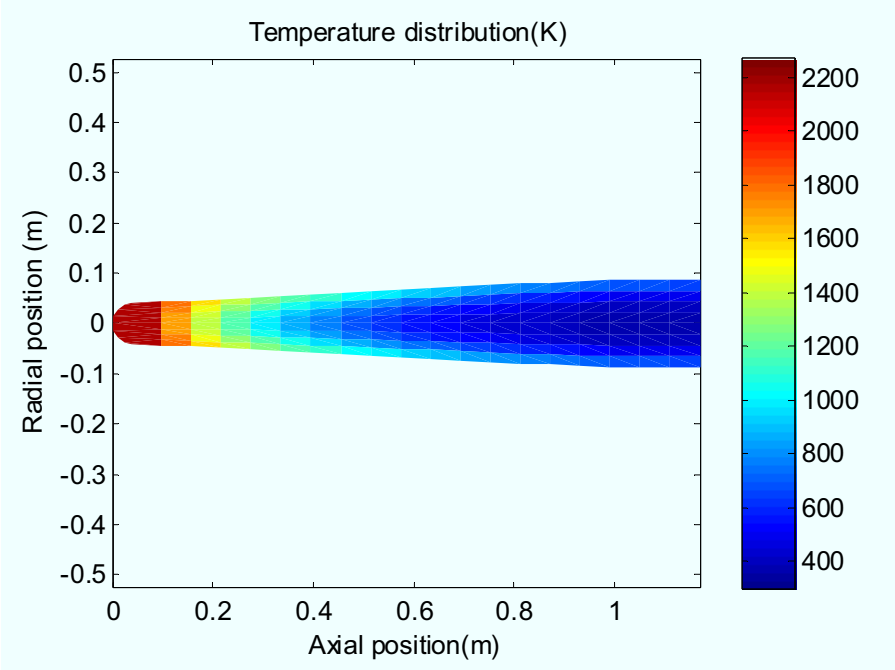

Figure 15: Baseline missile nose temperature distribution at end of flight

The missile exhibits satisfactory velocity with a cruise speed starting at Mach 3.5 and then slowly rising to Mach 5. The desired range of 100 km is achieved in 100.52 sec.

4.2 Fin span sensitivity analysis

The baseline fin span of 0.35 m was chosen arbitrarily. To investigate the effect of the fin span on the overall missile, a sensitivity analysis was performed. The sensitivity analysis involved varying the fin span from 0.15 to 0.45 m and monitoring the missile performance. Results are presented in Figure 16.

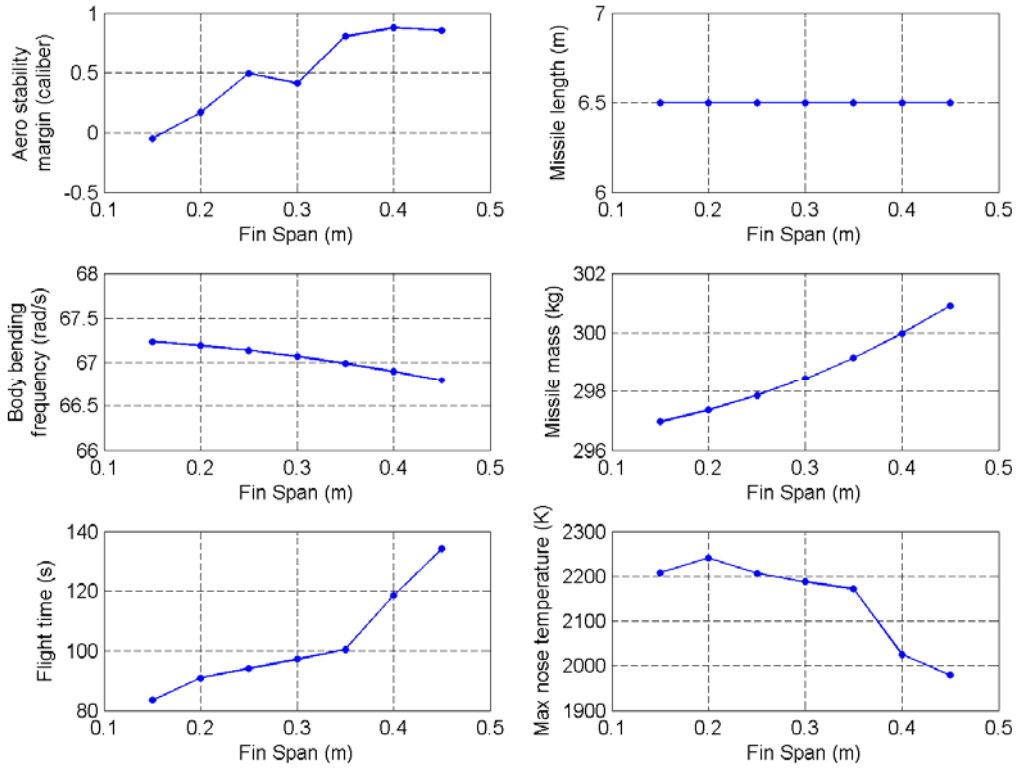

Figure 16: Effect of variation of fin span on missile characteristics and performance.

Figure 16 shows that increasing fin span increases the aerodynamic stability margin. Stability threshold is obtained for a fin span of 0.15 m. Increasing the fin span slightly increases the overall missile mass which in turn has an impact on the structure bending frequency. These effects are rather small.

Larger fin span induces more drag. The effect of the drag is observed indirectly by a longer flight time. A longer flight time means slower velocity with less aerodynamic heating and a lower nose temperature elevation.

4.3 Cruise altitude sensitivity analysis

The proposed baseline missile is designed to fly through a series of waypoints. These waypoints define a cruise altitude which affects drag force and, for airbreathing propulsion, propulsion efficiency. A higher cruise altitude also minimizes aerodynamic heating due to reduced air density. Although the current model employs a solid rocket motor that operates independently of the atmosphere, the cruise altitude still has an impact on the flight time as shown in Figure 17.

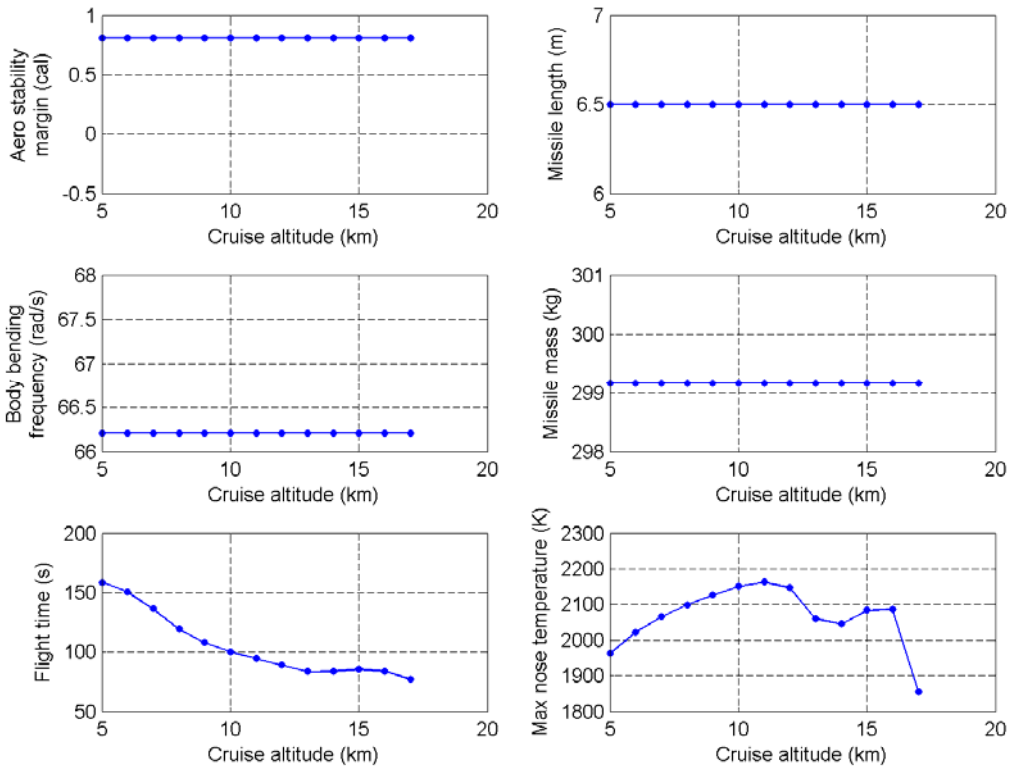

Figure 17: Effect of variation of cruise altitude on missile characteristics and performance.

Flying at higher altitude leads to a reduced flight time. However, the impact of flight altitude on nose temperature is less predictable. When the cruise altitude is raised from 5 to 10 km, it appears that the velocity increase, even coupled to lower air density, creates more aerodynamic heating as observed by the augmentation of the nose temperature. However, if the altitude is raised again from 10 to 15 km, the reduction in air density has more effect than the increase in velocity which reduces the nose temperature.

For cruise altitudes of 17 km and above, the reduction in air density creates a problem to the aerodynamic control of the missile. The autopilot and guidance do not succeed at maintaining the missile at the commanded altitude as shown in Figure 18. The observed near-ballistic trajectory has minimal impact for the rocket propelled missile studied here. However, for an airbreathing

missile, it can be anticipated that the manoeuvring authority to maintain the missile at its optimum flying altitude might be a problem.

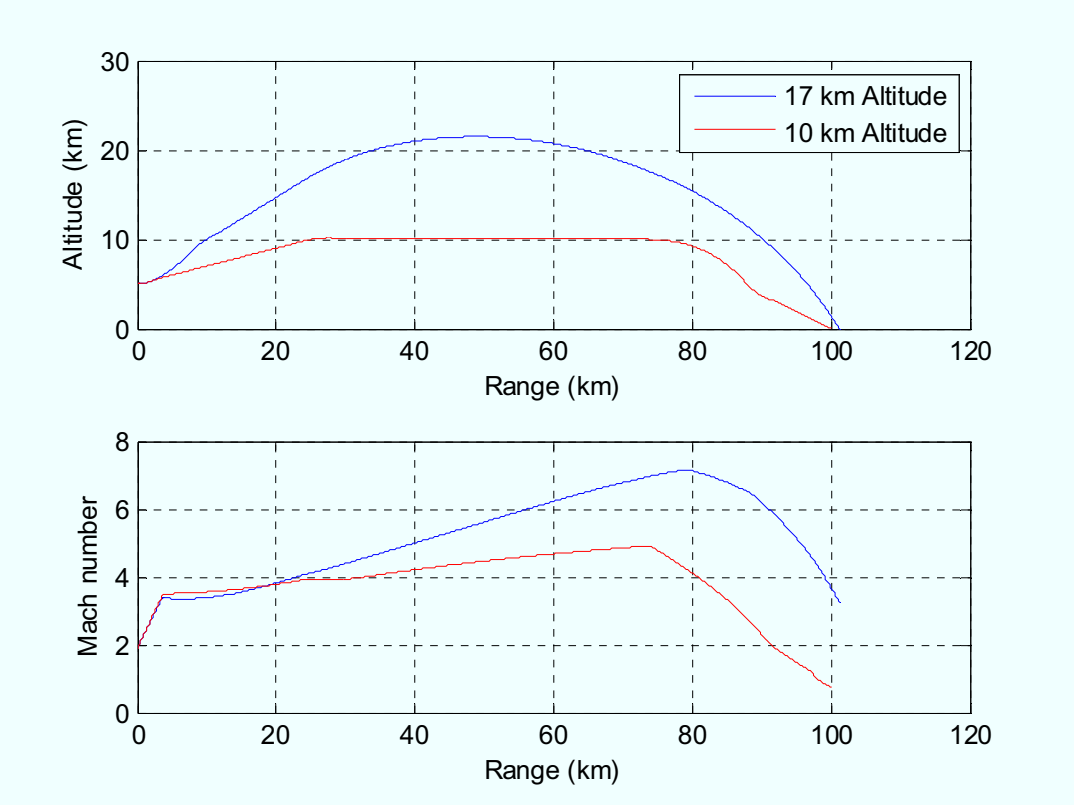

Figure 18: Trajectory and velocity profiles for a commanded cruise altitude of 10 km and 17 km.

Obviously, missile characteristics such as mass, length and stability are independent of cruise altitude.

4.4 Nose bluntness sensitivity analysis

Because hypersonic missiles are subject to high aerodynamic heating loads, care should be taken to ensure that the leading edge and the nose material can withstand the heat.

The tool used in this study permits to vary the nose bluntness radius of the missile to evaluate the overall effect on the missile flight time and the maximum temperature on the nose.

Figure 19 presents simulation results for nose radiuses ranging from 10 to 50 mm. The nose radius has small effect on the missile mass, structure and stability. However, an important trade-off is required between the flight time and the maximum nose temperature. A small nose radius improves the flight time by reducing drag but generate very high temperatures which are likely to exceed material resistance.

The minimum feasible radius is likely to be constrained by the temperature that the nose material can withstand.

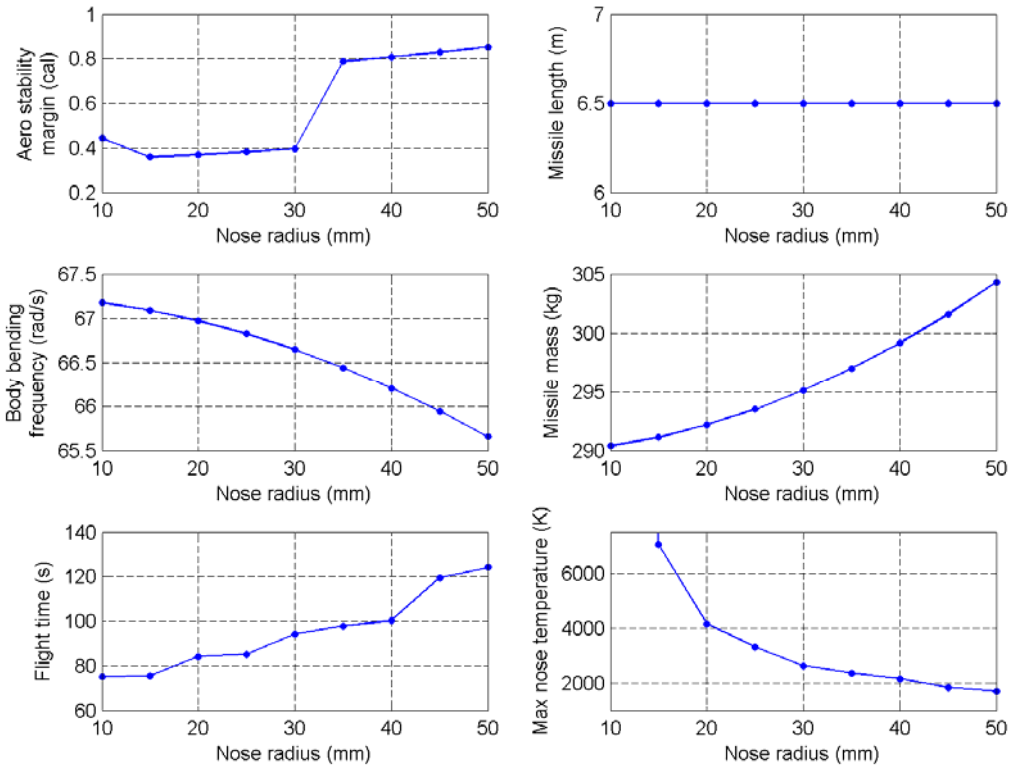

Figure 19: Effect of nose bluntness radius on missile characteristics and performance.

4.5 Skin thickness sensitivity analysis

The missile skin is the element that gives the missile its structural stiffness. Stiffness is required to prevent aeroelastic instability and maintain structural integrity.

Figure 20 shows the effect of varying the missile skin thickness.

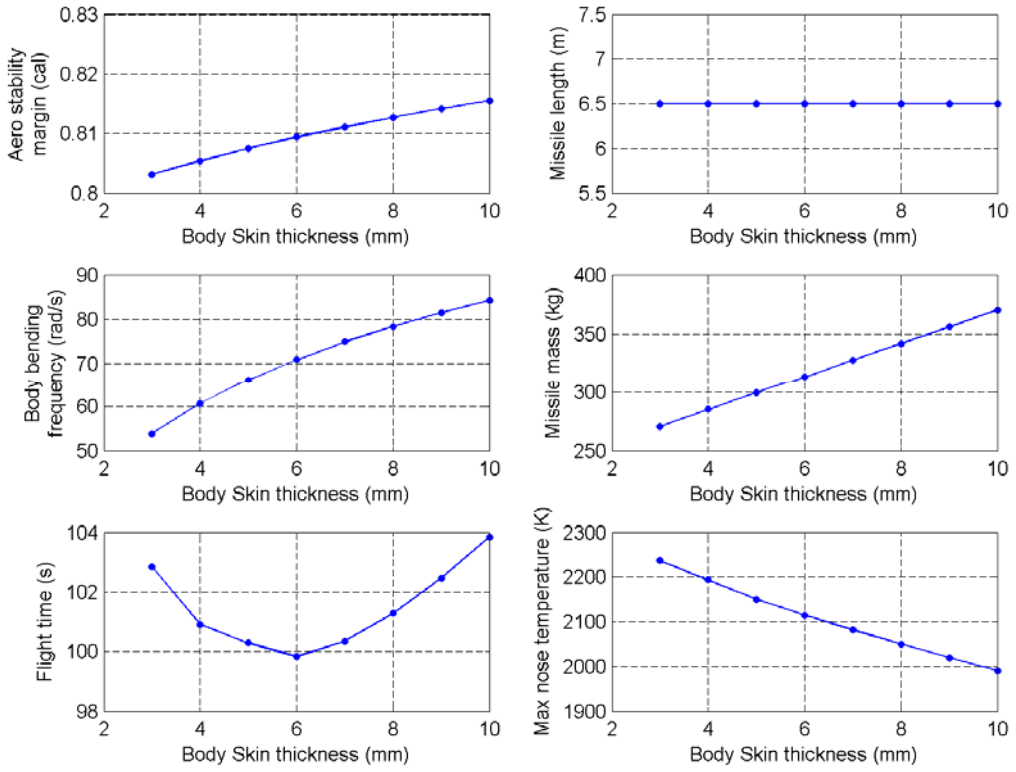

Figure 20: Effect of body structural skin thickness on missile characteristics and performance.

Changing the skin thickness has a small effect on the aerodynamic stability margin due to a small change in center-of-gravity location. Skin thickness directly influences the missile structure bending frequency and the missile mass.

One could expect that increasing thickness and missile mass would lead to a slower missile. However, the figure shows that a minimum flight time is achieved for a thickness of 6mm. Even if a lighter missile accelerates faster, the benefit of a faster velocity in the earlier flight phase is offset by an increased deceleration when the propulsion stops. This behaviour is clearly illustrated in Figure 21 where the same overall flight time is shown for 3 mm and 9 mm skin thickness. For the same flight time, a heavier 9 mm thick missile will have a more constant velocity. Lighter 3 mm thick missile exhibits a higher peak velocity which leads to higher temperature elevation due to aerodynamic heating and will lose velocity more quickly when propulsion stops.

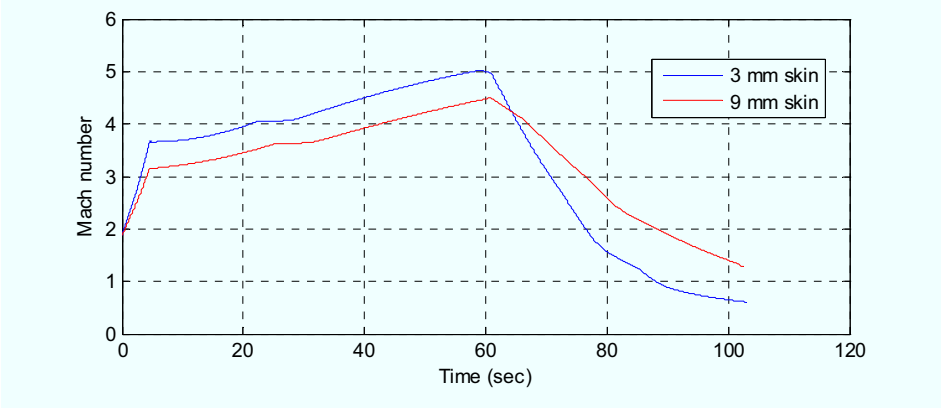

Figure 21: Comparison of speed for 3 mm and 9 mm body skin thickness.

It is expected that this behaviour is strongly dependent on the propulsion time-thrust curve. For the baseline missile, the propulsion stops at 60 s. This leaves the missile coasting using kinetic energy which is obviously better with a heavier missile.

4.6 Thrust profile trade-off

The thrust profile trade-off study aims at identifying the impact of the distribution of the rocket motor impulse between boost and sustain phases, and assesses the effect of the sustain thrust level. The boost thrust is not studied as it has not much impact since it will only vary the duration of the boost phase which is of short duration.

Since the total impulse of the motor is constant, the amount of impulse used for the boost phase influences the missile velocity at end of boost and the level of impulse available for sustainment of velocity. Given a level of impulse available for the sustainment, the level of sustain thrust directly affects the duration of the sustainment.

Since the boost impulse and the sustain thrust are coupled, a two-variable experimentation plan was designed to study the variation of these two variables simultaneously. The effect on the missile flight time is presented in Figure 22 while the effect on the maximum nose temperature is presented in Figure 23.

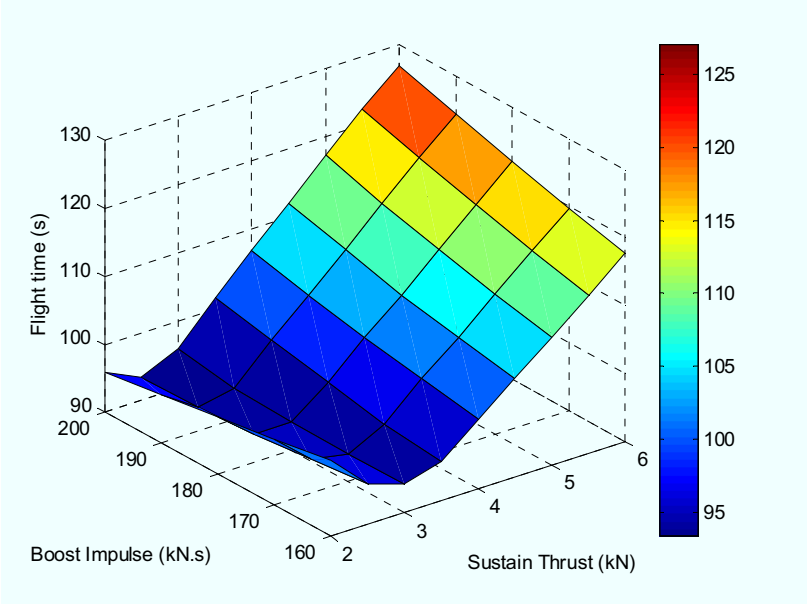

Figure 22: Effect of boost impulse and sustain thrust on missile flight time.

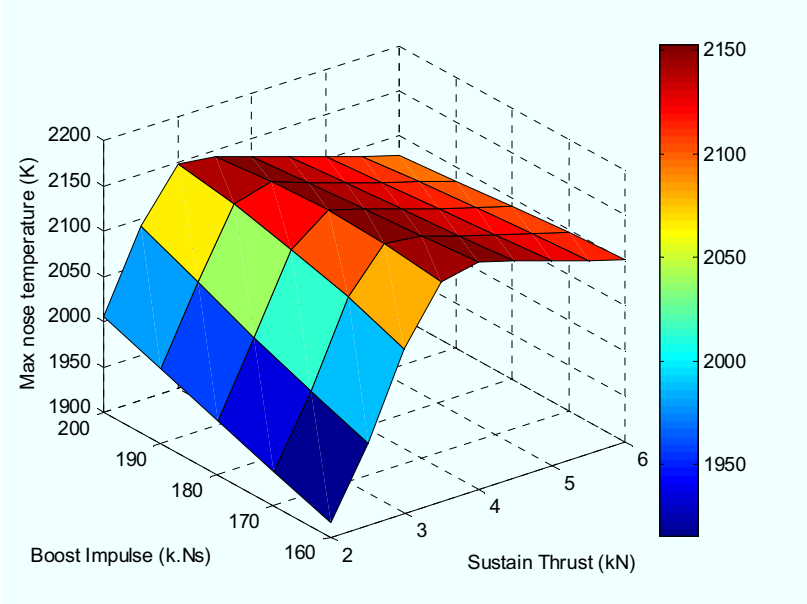

Figure 23: Effect of boost impulse and sustain thrust on maximum nose temperature.

Results show that several boost impulse and sustain thrust combinations give similar good flight time in the range of 94 s. The common characteristic between these solutions is that the end of the sustain phase coincide with the end of the engagement. To optimize the propulsion thrust profile to minimise flight time, it is thus essential to match the thrust duration to the flight time.

Since flight time is dependent on the engagement range (fixed here), a capacity to throttle the sustain thrust would be required to optimize the flight time for an arbitrary engagement range.

4.7 Missile size trade-off

Missile size, primarily defined by its length and diameter, is a key factor defining the time-space-velocity envelope that a missile can reach.

A parametric study is performed here to evaluate the impact of the missile dimensions on the flight time and nose temperature. To maintain aerodynamic stability within appropriate margin when the missile is resized, a fin span equal to twice the missile diameter is used.

Figure 24 presents the flight time for different missile lengths and diameters. It is observed that increasing both dimensions leads to a reduction of the flight time. However, the reduction in flight time becomes marginal when the missile reaches 421 kg at a length of 7.5 m and a diameter of 0.2 m as shown in Figure 25. This is explainable since the motor boost impulse and sustain thrust is not adjusted to take into account the larger missile dimensions. It is thus important to adjust the thrust profile when the missile is resized.

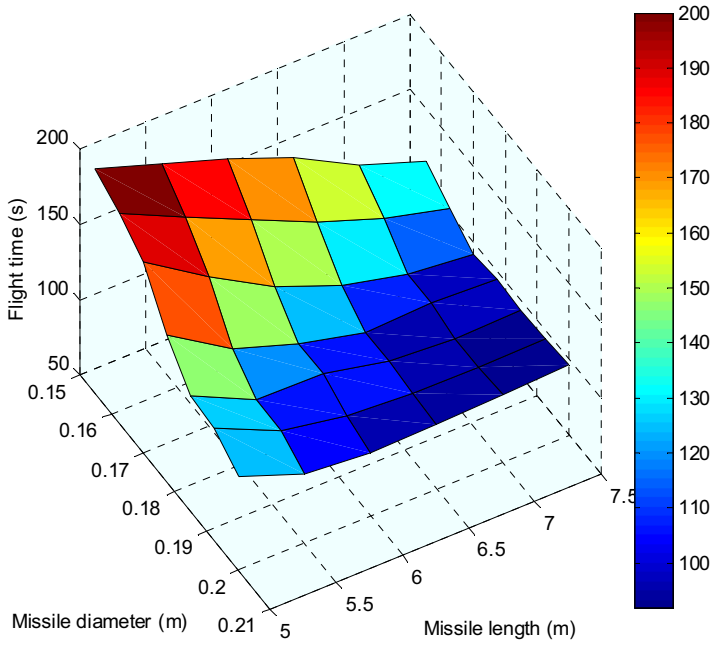

Figure 24: Effect of missile length and diameter on flight time.

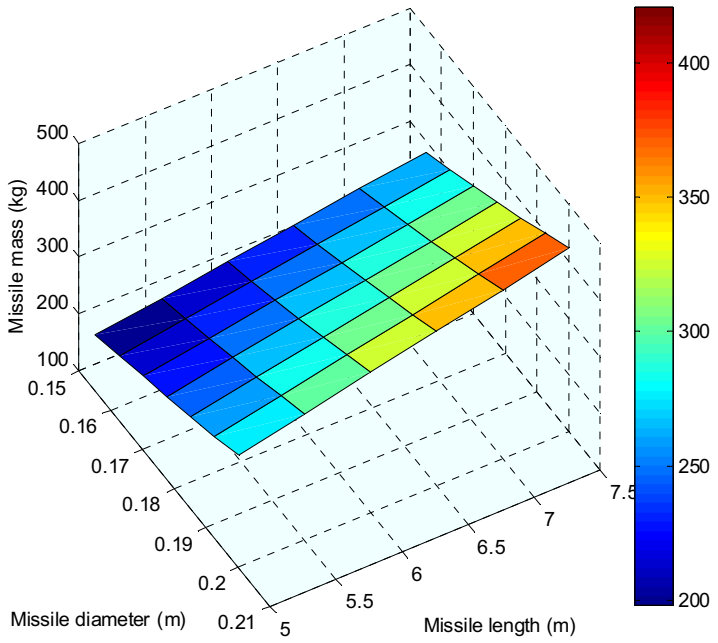

Figure 25: Effect of missile length and diameter on missile mass.

Figure 26 presents the maximum nose temperature for different missile lengths and diameters.

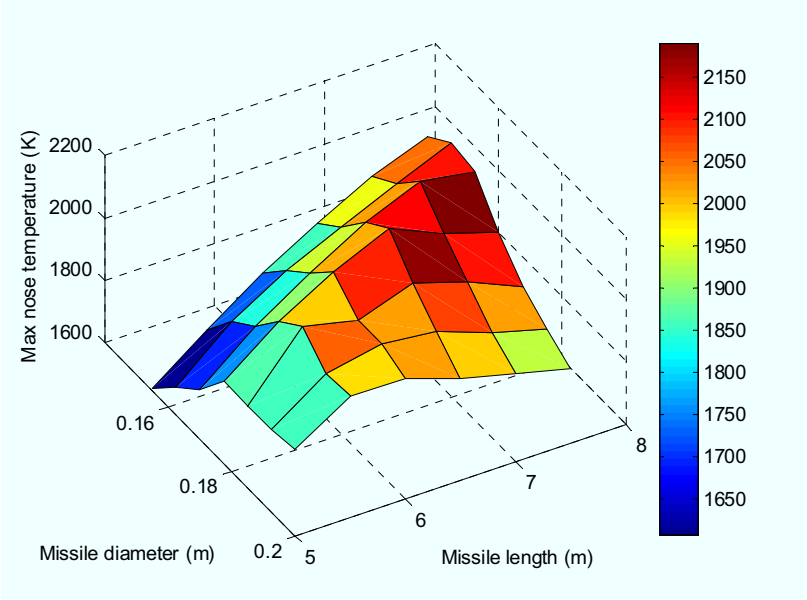

Figure 26: Effect of missile length and diameter on maximum nose temperature.

4.8 Summary of interaction observed in sensitivity analyses

The various sensitivity and trade-off analyses performed on key missile design variables allowed to observe several interesting interactions and learn key lessons to apply to the design and analysis of hypersonic missiles. These are:

- heating peaks at highest velocity even if it coincides with lowest air density at highest altitude. When the missile dives toward the surface target, the increase in drag created by higher atmospheric density creates a deceleration. Impact of deceleration on aerodynamic heating is larger than the effect of increased density;
- although heating is decreased, nose temperature continues to increase until velocity decreases below Mach 1.5;
- small fin span shall be used to minimize drag. Minimum fin span is limited by the aerodynamic stability margin;
- flying at higher altitude leads to a reduced flight time;
- for a cruise altitude of 17 km and above, the reduction in air density creates problem to the aerodynamic control of the missile. The autopilot and guidance do not succeed at maintaining the missile on the commanded flight path altitude. For an airbreathing missile, it can be anticipated that the manoeuvring authority to maintain the missile at its optimum flying altitude might be a problem for a conventional control system;
- small nose radius improves the flight time but generates very high temperatures which are likely to exceed material resistance;
- when missile mass and length is changed, it is important to adjust the propulsion thrust profile so that the end of the sustain phase coincides with the end of the engagement. To optimize the propulsion thrust profile to minimise flight time, it is thus essential to match the thrust duration to the flight time;
- since flight time is dependent on the engagement range (fixed here), a capacity to throttle the sustain thrust would be required to optimize the flight time for an arbitrary engagement range.

5 Optimization analysis

To demonstrate the application of optimization techniques to the design of hypersonic missiles, a simple time of flight optimization problem is presented here. The problem consists of minimizing the time of flight by varying independent missile design input variables. Design constraints are also applicable. Table 8 summarizes the optimization problem.

Table 8: Missile optimization problem

Objective: Minimize: Time of flight (s)				
Design Constraints				
		Missile mass (kg)	<	350
		Final nose temperature (K)	<	2200
Input variable bounds				
0.15	<	Diameter (m)	<	0.2
4	<	Missile length (m)	<	7.5
100 000	<	Boost impulse (N.s)	<	260 000
1250	<	Sustain thrust (N)	<	6 000
0.01	<	Nose radius (m)	<	0.05
5000	<	Cruise altitude (m)	<	15 000

To perform optimization, the Matlab Optimization Toolbox function FMINCON [25] was used. Table 9 presents the initial values compared to the optimum found. Detailed results are presented in Annex A.

Time of flight was significantly reduced from 100.52 s to 77.18 s. Compared to baseline missile, the most significant change is the reduction of the propulsion sustain thrust. This allows maintaining a uniform velocity close to Mach 5 during the complete flight. The baseline missile sustain propulsion was providing too much thrust, the missile continuing to accelerate during the sustain phase. The sustain phase was ending before the end of the flight and the missile was loosing significant velocity during a coasting phase, a phase that is eliminated with the optimized missile. Missile dimensions and mass differences between the baseline and optimum are not large.

The history of the solution investigated during the optimization process is shown on Figure 27. Optimization takes about one day to run using a Workstation with a 3.60GHz Intel Pentium 4 Processor.

Figure 28 to Figure 32 show various results of the optimized missile configuration.

Table 9: Missile optimization results

VARIABLES	Baseline	Optimum
Inputs		
Missile diameter (m)	0.175	0.1863
Missile length (m)	6.5	5.042
Boost impulse (Ns)	160 000	260 000*
Sustain thrust (N)	4000	1271
Nose radius (m)	0.04	0.0379
Cruise altitude (m)	10 000	15 000*
Outputs		
Time of flight (s)	100.52	77.18
Final nose temperature (K)	2171	2188*
Stability Margin (ϕ)	0.806	0.627
Missile mass (kg)	299.2	272.16
Natural bending frequency (rad/s)	66.99	112.9

*Active optimization constraints are boost impulse upper bound, nose temperature upper bound and cruise altitude upper bound. Values are within tolerance set in optimization algorithm.

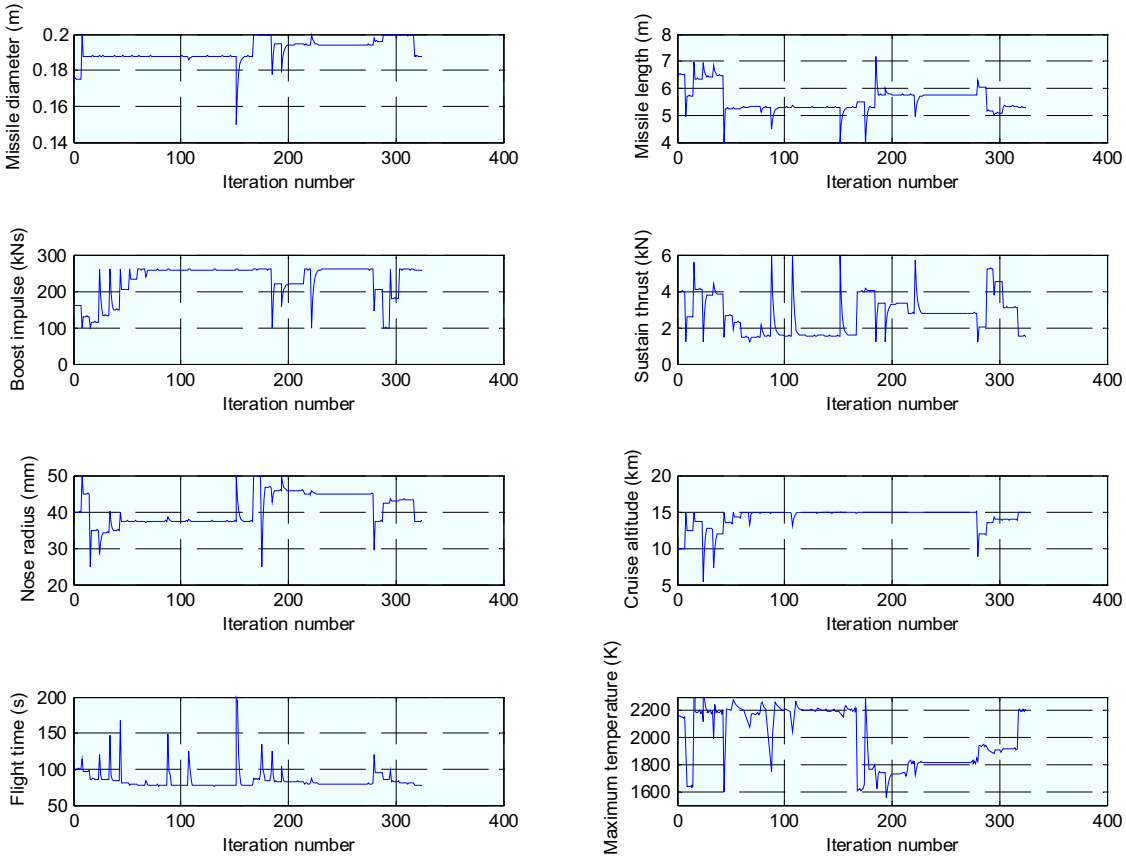

Figure 27: Optimization evolution

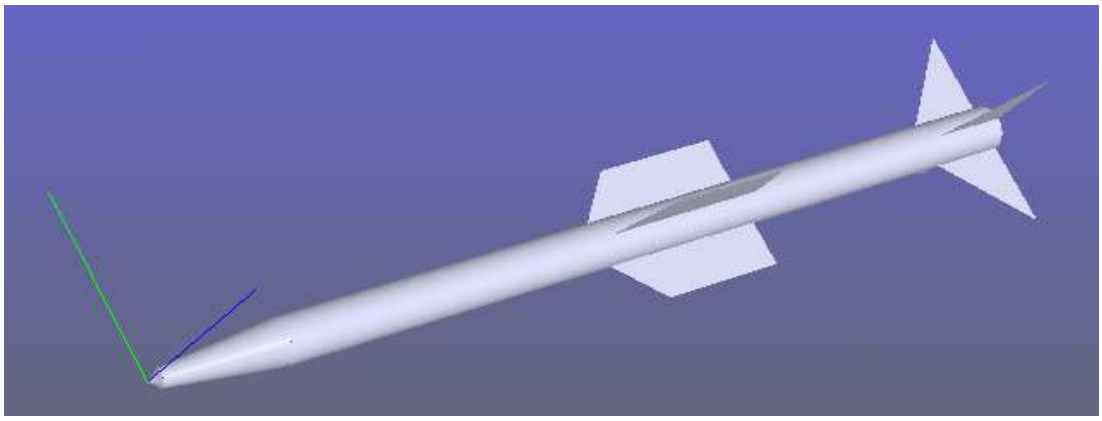

Figure 28: Illustration of optimum geometry

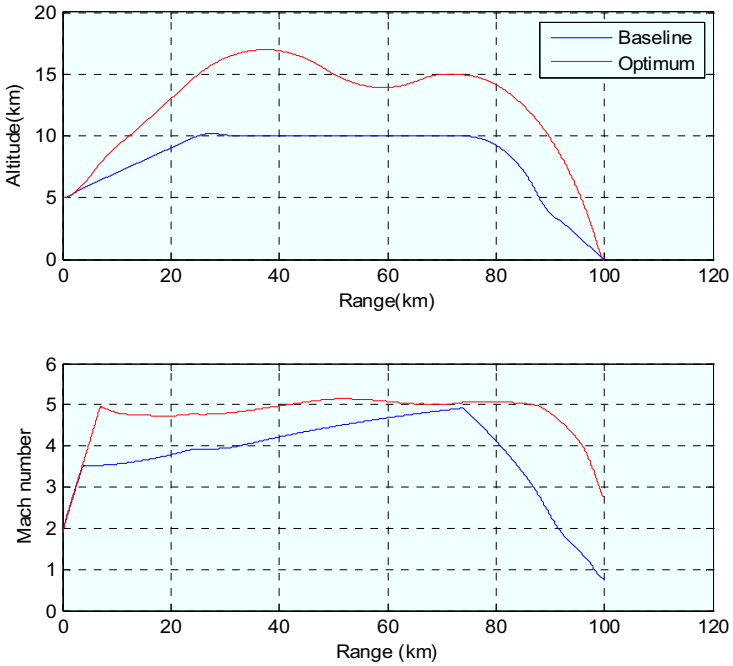

Figure 29: Optimum missile altitude and velocity as a function of range.

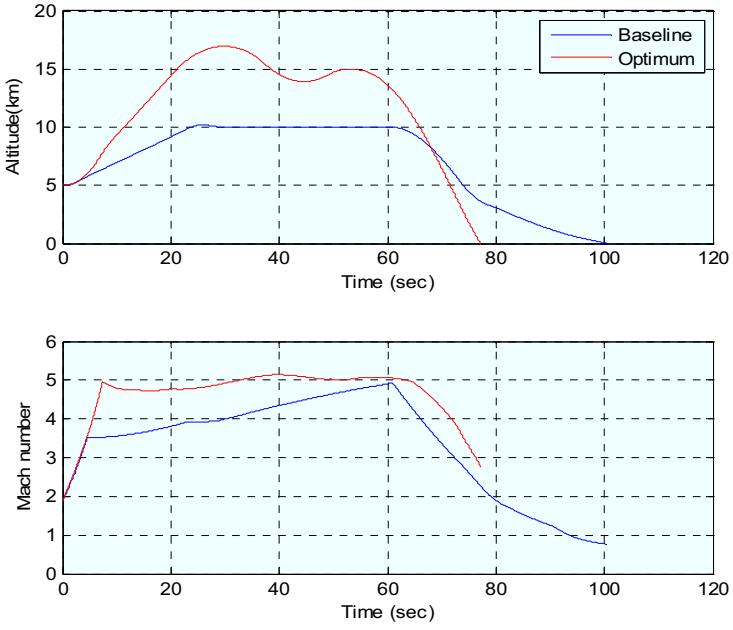

Figure 30: Optimum missile altitude and velocity as a function of time.

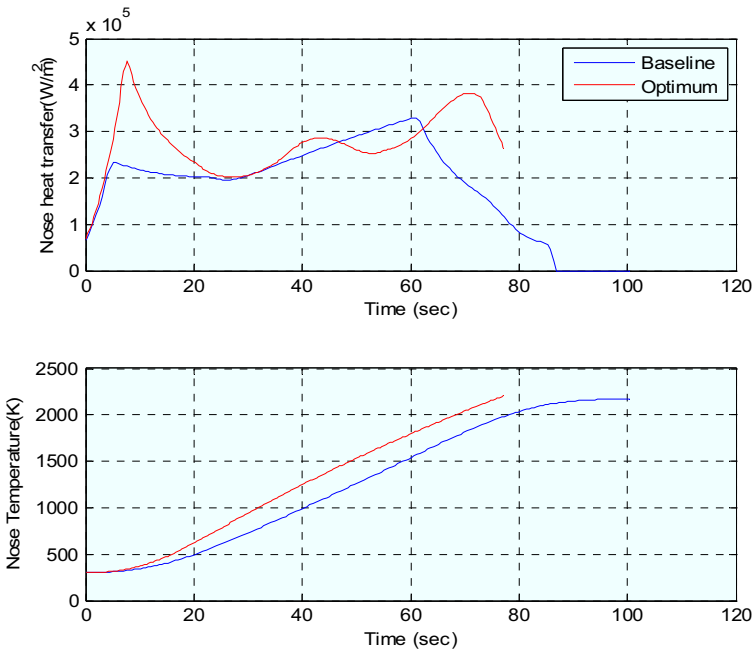

Figure 31: Optimum missile nose heat transfer and temperature evolution during flight.

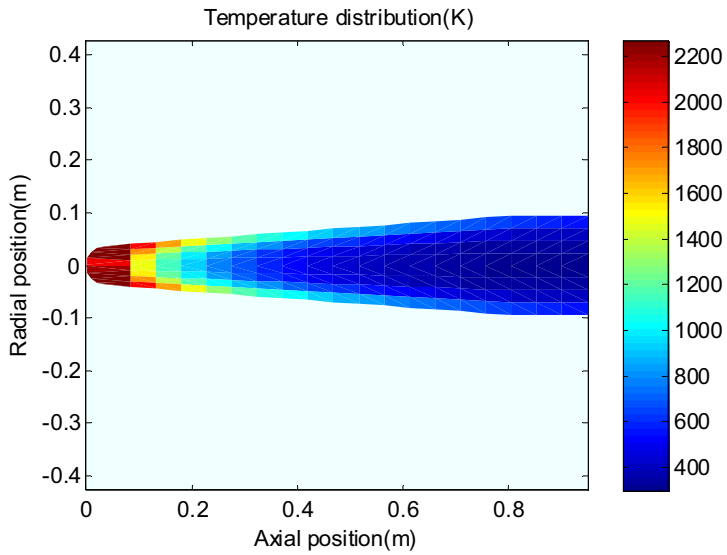

Figure 32: Optimum missile nose temperature distribution at end of flight.

Significant work was required to allow the optimization algorithm to converge. Experience showed that it is important to normalize the values of independent input optimization variables to allow the optimization algorithm to adequately take into account the effect of each variable. Robustness of the simulation model is also important. Optimization algorithms are prone to

exploit models with variables that make no sense. The optimization crashed several time due to models being operated outside of their intended envelop. When any models crashes or fails during the optimization, it is impossible to restart the optimization algorithm where it stopped.

6 Current deficiencies and limitations

Results presented in this document give an indication of the typical analyses that can be performed with the Multidisciplinary integrated analysis for engagement simulation of hypersonic weapons tool. However, the tool is not mature yet and presents significant deficiencies and limitations that would have to be addressed in the future. They are discussed in this section.

6.1 Subsystem models coverage

The tool presents basic analysis capabilities for all subsystems critical to the study of hypersonic weapon systems. However, it lacks an airbreathing propulsion model. The solid rocket motor propulsion model currently used is adequate to represent a booster but is not the typical cruise propulsion type for a high-speed missile.

An airbeathing propulsion model such as a ramjet or a scramjet would be much more relevant for the type of application sought. That would also require the addition of an air inlet that would create more aerodynamic-propulsion-structure coupling complexity.

The current tool is limited to axi-symmetric missile configurations. Support of wave-rider type configuration would be beneficial. This would require significant change to most subsystem models.

6.2 Fidelity and details of subsystems models

The individual level of details and the fidelity of the models presented in this document are in general low. This creates limitations that are discussed below. The benefits come from their integration in a single tool that allows subsystem interaction to be taken into account.

1. External geometry and mass estimation.

   Although simple, the nose-body-fins configuration can represent most axi-symmetric missile configurations. The level of details is correct although the configuration coverage limitations identified in section 6.1 apply (non-symmetric and wave-rider configurations). Mass estimation and geometry definition based on a detailed computer-aided-design (CAD) drawing would allow mitigating this limitation.

2. Aerodynamic prediction.

   Aerodynamic prediction is performed by Missile Datcom. Accuracy of prediction is not high but sufficient for current application. A computational-fluid-dynamic (CFD) prediction code that automatically meshes a CAD drawing would provide the best flexibility.

3. Internal components definition.

   The Internal Missile Component Definition subsystem lacks any relation between volume, density and function. Seeker, control actuation system and warhead volume and density are dependent on the technology used and their intended usage. Different types of seeker or actuator require different volumes. Guidelines to define required volume and density would be required to prevent user from entering unrealistic values. Similarly for the warhead, if the warhead payload is imposed, it drives the missile design. However, in some case, it could be desirable to have a payload model that allows performing design trade-off of payload size versus guidance accuracy for example.

4. Aerodynamic heating, structure heat transfer and conduction.

   The current tool provided only localized information on nose heating. To be practical, this function should be extended to other critical areas such as fins and intake leading edges. Currently, both the Aerodynamic Heating and the Conduction and Structure Temperature subsystem cannot handle these problems.

5. Structure first mode bending frequency.

   Estimation of the first mode bending frequency does not replace a detailed aero-servo-elastic analysis. Interaction of other structural and autopilot models can also lead to unstable interaction behaviors.

6.3 Use and deployment of large-scale architecture

The use of the commercial integration tool ModelCenter was very efficient to connect the various subsystem models. Also, sensitivity analysis and optimization tools were very efficient to perform studies and explore the results.

The multidisciplinary nature of the hypersonic missile system studies requires the help of subject matter experts in several science domains. Ideally, the subject matter experts should be themselves users of ModelCenter to develop models and study their respective subsystems. That would require several licenses of ModelCenter which creates significant deployment and maintenance cost.

The current work was performed in isolation by a small team of analysts and programmers that build the integrated analysis tool by integrating existing subsystem models and developing tools of minimal capabilities when no existing tool existed. The idea was to allow for later integration of high-fidelity models. Because of the limited accessibility to ModelCenter by the subject matter experts, limited further development occurred.

7 Conclusions

A multidisciplinary integrated analysis tool has been developed to study the problematic and challenges specific to hypersonic weapon systems. Various subsystem models were integrated to allow performing trade-off studies while considerating subsystem interactions.

A baseline missile reference was established as a starting point on which the impact of various design variables was assessed. The various sensitivity and trade-off analyses performed on key missile design variables allowed observing several interesting interactions and learning key lessons to apply to the design and analysis of hypersonic missiles.

To demonstrate the application of optimization techniques to the design of hypersonic missiles, a simple time of flight optimization problem was presented. Time of flight was significantly reduced by adjusting the propulsion sustain duration to match flight time. Missile dimensions and mass differences between the baseline and optimum were not large.

The tool presents basic analysis capabilities for all subsystems critical to the study of hypersonic weapon systems. Most subsystem models are limited in fidelity and details and would benefit from improvements. The most significant deficiencies are the lack of airbreathing propulsion model and the non support of non-symmetric airframe configurations such as wave-riders. Support of wave-rider type configuration would require significant changes to most subsystem models.

References

[1] Kors, D. (1990), "Design Considerations for Combined Airbreathing-Rocket Propulsion Systems", AIAA-1990-5216, AIAA Second International Aerospace Planes Conference, 29-31 October, Orlando, Florida.

[2] Naidu, D.S., Buffington, J.L. and Banda, S.S. (1999), "Resurrection in Hypersonics: Why, What and When", AIAA-1999-4053, AIAA Guidance, Navigation, and Control Conference and Exhibit, Portland, Oregon, 9-11 August.

[3] Schmidt, D. (1993), "Integrated Control of Hypersonic Vehicles", AIAA-1993-5091, AIAA/DGLR Fifth International Aerospace Planes and Hypersonics Technologies Conference", 30 November-3 December, Munich, Germany.

[4] Hunt, J.L., Lawing, P.L., Marcum, D.C. and Cubbage, J.M. (1978), "Conceptual Study of Hypersonic Airbreathing Missiles", AIAA 78-6, AIAA 16th Aerospace Sciences Meeting, Huntsville, Alabama, 16-18 January.

[5] Lewis, M.J. (2003), "A Hypersonic Propulsion Airframe Integration Overview", AIAA 2003-4405, 39th AIAA/ASME/SAE/ASEE Joint Propulsion Conference and Exhibit. 20-23 July, Huntsville, Alabama.

[6] Stuckey, R.M. and Lewis, M.J. (1999), "Hypersonic Missile Requirements and Operational Tradeoff Studies", AIAA 99-4929, AIAA International Space Planes and Hypersonic Systems and Technologies Conference, 9th, Norfolk, Virginia, 1-5 November, Collection of Technical Papers (A99-45401 12-15).

[7] Stuckey, R. and M. Lewis (2003), "Hypersonic missile requirement and operational tradeoff studies" Journal of Spacecraft and Rockets, vol 40 (no 2).

[8] Starkey, R.P., Rankins, F. and Pines, D. (2005), "Coupled Waverider/Trajectory Optimisation for Hypersonic Cruise", AIAA 2005-530, 43rd AIAA Aerospace Sciences Meeting and Exhibit, 10 - 13 January, Reno, Nevada

[9] Starkey, R.P., Rankins, and Pines, D. (2006), "Effects of Hypersonic Cruise Trajectory Optimisation Coupled with Airbreathing Vehicle Design", AIAA 2006-337, 44th AIAA Aerospace Sciences Meeting and Exhibit, 9 - 12 January, Reno, Nevada.

[10] Moerel, J.L.P.A. and Halswijk, W.H.C. (2005), "System Analysis of High Speed, Long Range Weapon Systems", AIAA 2005-5819, AIAA Atmospheric Flight Mechanics Conference and Exhibit, 15 - 18 August, San Francisco, California

[11] Couture, D., deChamplain, A., Stowe, R.A., Harris, P.G., Halswijk, W.H.C. and Moerel, J.L.P.A. (2008), "Comparison of Scramjet and Shcramjet Propulsion for an Hypersonic Waverider Configuration", AIAA 2008-5171, 44th AIAA/ASME/SAE/ASEE Joint Propulsion Conference and Exhibit, 21 - 23 July, Hartford, Connecticut.

[12] Mayer, A.E.H.J, Halswijk, W.H.C., Komduur, H.J., Lauzon, M. and Stowe, R.A. (2005), "A Modular Ducted Rocket Missile Model for Threat and Performance Assessment", AIAA 2005-6013, AIAA Modeling and Simulation Technologies Conference, 15-18 August, San Francisco, California.

[13] Doolan, C.J. (2006), "An Air-Launched Hypersonic Vehicle Performance Model", AIAA 2006-222, 44th AIAA Aerospace Sciences Meeting and Exhibit, 9 - 12 January, Reno, Nevada.

[14] Bowcutt, K.G., Kuruvila, G., Grandine, T.A., Hogan, T.A. and Cramer, E.J. (2008), "Advancements in Multidisciplinary Design Optimisation Applied to Hypersonic Vehicles to Achieve Closure", AIAA 2008-2591, 15th AIAA International Space Planes and Hypersonic Systems and Technologies Conference, 28 April - 1 May, Dayton, Ohio.

[15] Baker, M.L., Munson, M.J., Duchow, E., Hoppus, G.W. and Alston, K.Y. (2004), "System Level Optimisation in the Integrated Hypersonic Aeromechanics Tool (IHAT)", AIAA 2003-0618, 42nd AIAA Aerospace Sciences Meeting and Exhibit, Reno, Nevada, 5-8 January.

[16] Xianyu, W., Lin, X., Liang, J., Shibin, L., Xiaoqian, C. and Zhenguo, W. (2006), "The MDO Environment for Hypersonic Vehicle System Design and Optimisation", AIAA 2006-5191, 42nd AIAA/ASME/SAE/ASEE Joint Propulsion Conference and Exhibit, 9 - 12 July, Sacramento, California.

[17] Phoenix Integration Inc., "PHX ModelCenter", http://www.phoenix-int.com/software/phx_modelcenter.php, Accessed 13 August 2009.

[18] Spiegel, M.R. (1974), "Mathematical Handbook of Formulas and Tables", McGraw-Hill, New York.

[19] Blake, W.B. (1998), "Missile Datcom User s Manual 1997 Fortran 90 Revision" . AFRL-VAWP- TR-1998-3009.

[20] Lestage, R., Lauzon, M. and Jeffrey, A.J. (2001), "Automatic Tuning of Gain-Scheduled Autopilot for Computer Simulations", DREV-TR-2001-230.

[21] Nusca, M.J. (1990), "Supersonic/Hypersonic Aerodynamics and Heat Transfer for Projectile Design Using Viscous-Inviscid Interaction" . BRL-TR-3119. Ballistics Research Laboratory, Aberdeen Proving Ground, Maryland.

[22] Nusca, M.J. (1991), "Aerothermodynamics Analysis for Axisymmetric Projectiles at Supersonic/Hypersonic Speeds" . AIAA 9th Applied Aerodynamics Conference, AIAA 91-3257, 23-25 September.

[23] Parisé, N. (2007), "Evaluation of Aerodynamic Software in the Hypersonic Flow Regime", DRDC Valcartier CR 2007-247.

[24] Parisé, N (2005). “Aerodynamic heating software evaluation”, DRDC Valcartier CR 2005-333.

[25] The Mathworks Inc., “Optimisation Toolbox User's Guide”, http://www.mathworks.com/access/helpdesk/help/pdf_doc/optim/optim_tb.pdf, Accessed 18 September 2009.

Annex A Baseline and optimized missile system definition

A.1 External Geometry Definition

Variable	Baseline Value	Optimized Value	Units	Description
ExternalGeometry.AxisymmetricBody1.LNOSE	0.975	0.7563	m	Nose length
ExternalGeometry.AxisymmetricBody1.DNOSE	0.175	0.1863	m	Nose diameter
ExternalGeometry.AxisymmetricBody1.BNOSE	0.04	0.03792	m	Nose bluntness radius
ExternalGeometry.AxisymmetricBody1.LCENTR	5.525	4.28573	m	Body length
ExternalGeometry.AxisymmetricBody1.DCENTR	0.175	0.1863	m	Body diameter
ExternalGeometry.AxisymmetricBody1.DatcomBodyStr	$AXIBOD LNOSE = 0.9750, DNOSE = 0.1750, BNOSE = 0.0400, LCENTR = 5.5250, DCENTR = 0.1750, DEXIT = 0.1750, $END	$AXIBOD LNOSE = 0.7563, DNOSE = 0.1863, BNOSE = 0.03792, LCENTR = 4.28573, DCENTR = 0.1863, DEXIT = 0.1863, $END		Datcom String for geometry definition
ExternalGeometry.AxisymmetricBody1.BodyThickness	0.0045	0.005	m	Body thickness
ExternalGeometry.AxisymmetricBody1.LengthMissile	6.5	5.04203	m	Length of missile
ExternalGeometry.AxisymmetricBody1.BodyMaterialDensity	4000	4000	kg/m^3	Body material density
ExternalGeometry.FinSet1.SSPAN1	0.0875	0.09315	m	Fin span from center line to base
ExternalGeometry.FinSet1.SSPAN2	0.4375	0.46575	m	Fin span from center line to tip
ExternalGeometry.FinSet1.CHORD1	0.35	0.3726	m	Fin chord length at base
ExternalGeometry.FinSet1.CHORD2	0.01	0.01	m	Fin chord length at tip
ExternalGeometry.FinSet1.SWEEP	0.01	0.01	deg	Fin sweep angle
ExternalGeometry.FinSet1.XLE	6.15	4.66943	m	Fin trailing edge distance from nose
ExternalGeometry.FinSet1.DatcomFinSet1Str	$FINSET1 NPANEL = 4., SECTYP = HEX, SSPAN = 0.0875,0.4375, CHORD = 0.3500,0.0100, SWEEP = 0.0100,0., XLE = 6.1500, STA = 2*1., $END	$FINSET1 NPANEL = 4., SECTYP = HEX, SSPAN = 0.0932,0.4658, CHORD = 0.3726,0.0100, SWEEP = 0.0100,0., XLE = 4.66943, STA = 2*1., $END	-	Datcom String for geometry definition
ExternalGeometry.FinSet1.FinSetNo	1	1		Fin set number
ExternalGeometry.FinSet1.FinThickness	0.004	0.004	m	Fin thickness
ExternalGeometry.FinSet1.FinMaterialDensity	2700	2700	kg/m^3	In material density
ExternalGeometry.FinSet2.SSPAN1	0.0875	0.09315	m	Fin span from center line to base
ExternalGeometry.FinSet2.SSPAN2	0.2625	0.27945	m	Fin span from center line to tip
ExternalGeometry.FinSet2.CHORD1	0.7	0.7452	m	Fin chord length at base
ExternalGeometry.FinSet2.CHORD2	0.525	0.5589	m	Fin chord length at tip

ExternalGeometry.FinSet2.SWEEP	0.01	0.01	deg	Fin sweep angle
ExternalGeometry.FinSet2.XLE	3.25	2.52101	m	Fin trailing edge distance from nose
ExternalGeometry.FinSet2.DatcomFinSet1Str	$FINSET2 NPANEL = 4., SECTYP = HEX, SSPAN = 0.0875,0.2625, CHORD = 0.7000,0.5250, SWEEP = 0.0100,0., XLE = 3.2500, STA = 2*1., $END	$FINSET2 NPANEL = 4., SECTYP = HEX, SSPAN = 0.09315,0.27945, CHORD = 0.7452,0.5589, SWEEP = 0.0100,0., XLE = 2.521, STA = 2*1., $END	-	Datcom String for geometry definition
ExternalGeometry.FinSet2.FinSetNo	2	2		Fin set number
ExternalGeometry.FinSet2.FinThickness	0.004	0.004	m	Fin thickness
ExternalGeometry.FinSet2.FinMaterialDensity	2700	2700	kg/m^3	Fin material density

A.2 Missile Datcom Aerodynamic Prediction

Variable	Baseline Value	Optimized Value	Units	Description
Aerodynamics.DatcomtoMatlabAxisymetric2Finsets.Geo1	$AXIBOD LNOSE = 0.9750, DNOSE = 0.1750, BNOSE = 0.0400, LCENTR = 5.5250, DCENTR = 0.1750, DEXIT = 0.1750, $END	$AXIBOD LNOSE = 0.7563, DNOSE = 0.1863, BNOSE = 0.03792, LCENTR = 4.28573, DCENTR = 0.1863, DEXIT = 0.1863, $END		Datcom String for geometry definition
Aerodynamics.DatcomtoMatlabAxisymetric2Finsets.Geo2	$FINSET1 NPANEL = 4., SECTYP = HEX, SSPAN = 0.0875,0.4375, CHORD = 0.3500,0.0100, SWEEP = 0.0100,0., XLE = 6.1500, STA = 2*1., $END	$FINSET1 NPANEL = 4., SECTYP = HEX, SSPAN = 0.0932,0.4658, CHORD = 0.3726,0.0100, SWEEP = 0.0100,0., XLE = 4.66943, STA = 2*1., $END		Datcom String for geometry definition
Aerodynamics.DatcomtoMatlabAxisymetric2Finsets.Geo3	$FINSET2 NPANEL = 4., SECTYP = HEX, SSPAN = 0.0875,0.2625, CHORD = 0.7000,0.5250, SWEEP = 0.0100,0., XLE = 3.2500,	$FINSET2 NPANEL = 4., SECTYP = HEX, SSPAN = 0.09315,0.27945, CHORD = 0.7452,0.5589, SWEEP = 0.0100,0., XLE = 2.521,		Datcom String for geometry definition

	STA = 2*1., #$END	STA = 2*1., $END		
Aerodynamics.DatcomtoMatlabAxisymetric2Finsets.Geo4	$REFQ SREF = 3.1416, LREF = 1., $END	$REFQ SREF = 3.1416, LREF = 1., $END		Datcom String for geometry definition
DatcomtoMatlabAxisymetric2Finsets.OperatingConditions.PhiTable	0, 22.5, 45	0, 22.5, 45	deg	Phi angle vector for aerodynamic table.
DatcomtoMatlabAxisymetric2Finsets.OperatingConditions.MachTable	0.5, 0.8, 0.95, 1, 1.2, 1.5, 3, 6	0.5, 0.8, 0.95, 1, 1.2, 1.5, 3, 6		Mach Number vector for aerodynamic table
DatcomtoMatlabAxisymetric2Finsets.OperatingConditions.DeltaTable	-15, 0, 15	-15, 0, 15	deg	Fin deflection angle vector for Aerodynamic Table
DatcomtoMatlabAxisymetric2Finsets.OperatingConditions.AOATable	0, 4, 8, 10	0, 4, 8, 10	deg	Alpha AOA vector for aerodynamic table

A.3 Internal Missile Component Definition

Variable	Baseline Value	Optimized Value	Units	Description
InternalComponents.CylinderWarhead.XLEfront	0.975	0.7563	m	Motor front end distance from nose
InternalComponents.CylinderWarhead.Diameter	0.175	0.1863	m	Motor diameter
InternalComponents.CylinderWarhead.Length	0.33	0.33	m	Length
InternalComponents.CylinderWarhead.Density	2400	2400	kg/m^3	Density
InternalComponents.CylinderWarhead.XLEend	1.305	1.0863	m	Motor rear end distance from nose
InternalComponents.CylinderGuidanceControl.XLEfront	0.04	0.03792	m	Motor front end distance from nose
InternalComponents.CylinderGuidanceControl.Diameter	0.08	0.07584	m	Motor diameter
InternalComponents.CylinderGuidanceControl.Length	0.935	0.71838	m	Length
InternalComponents.CylinderGuidanceControl.Density	2000	2000	kg/m^3	Density
InternalComponents.CylinderGuidanceControl.XLEend	0.975	0.7563	m	Motor rear end distance from nose

A.4 Solid Rocket Motor Propulsion

Variable	Baseline Value	Optimized Value	Units	Description
SolidRocketMotor.XLEfront	1	1.00841	m	Motor front end distance from nose
SolidRocketMotor.MotorLength	5.2	4.03363	m	Motor length
SolidRocketMotor.Diameter	0.175	0.1863	m	Motor diameter

SolidRocketMotor.PropellantDensity	1688	1688	kg/m^2	Propellant density
SolidRocketMotor.PropellantIsp	219	219	s	Propellant specific impulse
SolidRocketMotor.PropellantVolumeFraction	0.85	0.85		Propellant volume fraction
SolidRocketMotor.BoostThrust	35	35	kN	Motor thrust during boost phase
SolidRocketMotor.SustainThrust	4	1.27117	kN	Motor thrust during sustain phase
SolidRocketMotor.XLEend	6.2	5.04204	M	Motor rear end distance from nose
SolidRocketMotor.DesiredBoostImpulse	160	260	kN.s	Desired Boost phase impulse
SolidRocketMotor.TotalImpulse	385545	338936	N.s	Total impulse of motor
SolidRocketMotor.Motor.NozzleExitArea	0.02405	0.02726	m^2	Motor nozzle exit area
SolidRocketMotor.Motor.MotorMass	0, 0.001, 104.981164426571, 104.982164426571, 179.45653826, 179.45753826	0, 0.001, 36.7397345648084, 36.7407345648084, 157.76159204413, 157.76259204413	kg	thrust vs Rate MotorMassRemaining
SolidRocketMotor.Motor.ThrustSeaLevel	0, 4000, 4000, 35000, 35000, 0	0, 1271.17, 1271.17, 35000, 35000, 0	N	Thrust at sea level vector
SolidRocketMotor.Motor.SpecificImpulseMotor	219	219	s	Fuel Rate Spent

A.5 Airframe Physical Properties

Variable	Baseline Value	Optimized Value	Units	Description
AirframeCharacteristics.1.MassProperties.IsConsumable	0	0		Consumable material property
AirframeCharacteristics.1.MassProperties.CG_X	3.25	2.52101	m	CG X location wrt nose
AirframeCharacteristics.1.MassProperties.CG_Y	0	0	m	CG Y location wrt nose
AirframeCharacteristics.1.MassProperties.CG_Z	0	0	m	CG Z location wrt nose
AirframeCharacteristics.1.MassProperties.Volume	0.15634	0.13744	m^3	Volume
AirframeCharacteristics.1.MassProperties.SurfaceArea	3.57357	2.951	m^2	Surface Area
AirframeCharacteristics.1.MassProperties.Mass	64.3243	59.02	kg	Mass
AirframeCharacteristics.1.MassProperties.Ixx	0.49248	0.51211	kg.m^2	X axis polar moment of inertia wrt CG
AirframeCharacteristics.1.MassProperties.Iyy	226.476	125.035	kg.m^2	Y axis polar moment of inertia wrt CG
AirframeCharacteristics.1.MassProperties.Izz	226.476	125.035	kg.m^2	Z axis polar moment of inertia wrt CG
AirframeCharacteristics.2.MassProperties.CG_X	6.325	4.85573	m	CG X location wrt nose
AirframeCharacteristics.2.MassProperties.CG_Y	0	0	m	CG Y location wrt nose
AirframeCharacteristics.2.MassProperties.CG_Z	0	0	m	CG Z location wrt nose
AirframeCharacteristics.2.MassProperties.Volume	0.00101	0.00114	m^3	Volume
AirframeCharacteristics.2.MassProperties.SurfaceArea	0.504	0.57023	m^2	Surface Area
AirframeCharacteristics.2.MassProperties.Mass	2.7216	3.07923	kg	Mass
AirframeCharacteristics.2.MassProperties.Ixx	0.75014	0.96186	kg.m^2	X axis polar moment of inertia wrt CG
AirframeCharacteristics.2.MassProperties.Iyy	0.37507	0.48093	kg.m^2	Y axis polar moment of inertia wrt CG
AirframeCharacteristics.2.MassProperties.Izz	0.37507	0.48093	kg.m^2	Z axis polar moment of inertia wrt CG
AirframeCharacteristics.2.MassProperties.IsConsumable	0	0		Consumable material property
AirframeCharacteristics.3.MassProperties.IsConsumable	0	0		Consumable material property
AirframeCharacteristics.3.MassProperties.CG_X	1.435	1.435	m	CG X location wrt nose
AirframeCharacteristics.3.MassProperties.CG_Y	0	0	m	CG Y location wrt nose
AirframeCharacteristics.3.MassProperties.CG_Z	0	0	m	CG Z location wrt nose

AirframeCharacteristics.3.MassProperties.Volume	0.03522	0.03522	m^3	Volume
AirframeCharacteristics.3.MassProperties.SurfaceArea	1.12705	1.12705	m^2	Surface Area
AirframeCharacteristics.3.MassProperties.Mass	20.2869	20.2869	kg	Mass
AirframeCharacteristics.3.MassProperties.Ixx	0.07925	0.07925	kg.m^2	X axis polar moment of inertia wrt CG
AirframeCharacteristics.3.MassProperties.Iyy	13.9253	13.9253	kg.m^2	Y axis polar moment of inertia wrt CG
AirframeCharacteristics.3.MassProperties.Izz	13.9253	13.9253	kg.m^2	Z axis polar moment of inertia wrt CG
AirframeCharacteristics.4.MassProperties.CG_X	3.905	3.02523	m	CG X location wrt nose
AirframeCharacteristics.4.MassProperties.CG_Y	0	0	m	CG Y location wrt nose
AirframeCharacteristics.4.MassProperties.CG_Z	0	0	m	CG Z location wrt nose
AirframeCharacteristics.4.MassProperties.Volume	0.12507	0.10995	m^3	Volume
AirframeCharacteristics.4.MassProperties.SurfaceArea	2.85886	2.3608	m^2	Surface Area
AirframeCharacteristics.4.MassProperties.Mass	179.458	157.763	kg	Mass
AirframeCharacteristics.4.MassProperties.Ixx	0.68699	0.68445	kg.m^2	X axis polar moment of inertia wrt CG
AirframeCharacteristics.4.MassProperties.Iyy	404.721	214.244	kg.m^2	Y axis polar moment of inertia wrt CG
AirframeCharacteristics.4.MassProperties.Izz	404.721	214.244	kg.m^2	Z axis polar moment of inertia wrt CG
AirframeCharacteristics.4.MassProperties.IsConsumable	1	1		Consumable material property
AirframeCharacteristics.5.MassProperties.CG_X	1.14	0.9213	m	CG X location wrt nose
AirframeCharacteristics.5.MassProperties.CG_Y	0	0	m	CG Y location wrt nose
AirframeCharacteristics.5.MassProperties.CG_Z	0	0	m	CG Z location wrt nose
AirframeCharacteristics.5.MassProperties.Volume	0.00794	0.009	m^3	Volume
AirframeCharacteristics.5.MassProperties.SurfaceArea	0.18143	0.19314	m^2	Surface Area
AirframeCharacteristics.5.MassProperties.Mass	19.0499	21.5895	kg	Mass
AirframeCharacteristics.5.MassProperties.Ixx	0.07293	0.09367	kg.m^2	X axis polar moment of inertia wrt CG
AirframeCharacteristics.5.MassProperties.Iyy	0.20934	0.24276	kg.m^2	Y axis polar moment of inertia wrt CG
AirframeCharacteristics.5.MassProperties.Izz	0.20934	0.24276	kg.m^2	Z axis polar moment of inertia wrt CG
AirframeCharacteristics.5.MassProperties.IsConsumable	0	0		Consumable material property
AirframeCharacteristics.6.MassProperties.CG_X	0.5075	0.39711	m	CG X location wrt nose
AirframeCharacteristics.6.MassProperties.CG_Y	0	0	m	CG Y location wrt nose
AirframeCharacteristics.6.MassProperties.CG_Z	0	0	m	CG Z location wrt nose
AirframeCharacteristics.6.MassProperties.Volume	0.0047	0.00324	m^3	Volume
AirframeCharacteristics.6.MassProperties.SurfaceArea	0.23499	0.17115	m^2	Surface Area
AirframeCharacteristics.6.MassProperties.Mass	9.39967	6.48974	kg	Mass
AirframeCharacteristics.6.MassProperties.Ixx	0.00752	0.00467	kg.m^2	X axis polar moment of inertia wrt CG
AirframeCharacteristics.6.MassProperties.Iyy	0.68855	0.28143	kg.m^2	Y axis polar moment of inertia wrt CG
AirframeCharacteristics.6.MassProperties.Izz	0.68855	0.28143	kg.m^2	Z axis polar moment of inertia wrt CG
AirframeCharacteristics.6.MassProperties.IsConsumable	0	0		Consumable material property
AirframeCharacteristics.7.MassProperties.CG_X	0.68	0.68	m	CG X location wrt nose
AirframeCharacteristics.7.MassProperties.CG_Y	0	0	m	CG Y location wrt nose
AirframeCharacteristics.7.MassProperties.CG_Z	0	0	m	CG Z location wrt nose
AirframeCharacteristics.7.MassProperties.Volume	0.00196	0.00196	m^3	Volume
AirframeCharacteristics.7.MassProperties.SurfaceArea	0.06283	0.06283	m^2	Surface Area
AirframeCharacteristics.7.MassProperties.Mass	3.927	3.927	kg	Mass
AirframeCharacteristics.7.MassProperties.Ixx	0.00767	0.00767	kg.m^2	X axis polar moment of inertia wrt CG
AirframeCharacteristics.7.MassProperties.Iyy	0.01221	0.01221	kg.m^2	Y axis polar moment of inertia wrt CG
AirframeCharacteristics.7.MassProperties.Izz	0.01221	0.01221	kg.m^2	Z axis polar moment of inertia wrt CG
AirframeCharacteristics.7.MassProperties.IsConsumable	0	0		Consumable material property

AirframeCharacteristics.MassMissile	119.7092862, 299.16682446	114.392300968539, 272.154893012669	kg	Missile mass vector
AirframeCharacteristics.XCgMissile	2.37690158037213, 3.29354326047954	1.90565028005158, 2.5546447105795	m	Missile center of gravity vector
AirframeCharacteristics.IxxMissile	1.40998421446312, 2.09697010311469	1.65921329853419, 2.3436601908172	kg.m^2	Missile Ixx inertia vector
AirframeCharacteristics.IyyMissile	241.68610885491, 646.407254678436	139.977541281058, 354.221793586943	kg.m^2	Missile Iyy inertia vector
AirframeCharacteristics.IzzMissile	241.68610885491, 646.407254678436	139.977541281058, 354.221793586943	kg.m^2	Missile Izz inertia vector

A.6 Autopilot Tuning

Variable	Baseline Value	Optimized Value	Units	Description
Autopilot.accel	0.7	0.7		Closed loop acceleration factor, typically 1.5 for canard or tail, .75 for wing
Autopilot.OmegaOpenLoop	[7 x 3 matrix]	[7 x 3 matrix]	rad/s	airframe open loop natural frequency
Autopilot.Omega	[7 x 3 matrix]	[7 x 3 matrix]	rad/s	desired airframe closed loop bandwidth
Autopilot.AirframeCharacteristics.MassMissile	119.7092862, 299.16682446	114.392300968539, 272.154893012669	kg	Missile mass vector
Autopilot.AirframeCharacteristics.XCgMissile	2.37690158037213, 3.29354326047954	1.90565028005158, 2.5546447105795	m	Missile center of gravity vector
Autopilot.AirframeCharacteristics.IxxMissile	1.40998421446312, 2.09697010311469	1.65921329853419, 2.3436601908172	kg.m^2	Missile Ixx inertia vector
Autopilot.AirframeCharacteristics.IyyMissile	241.68610885491, 646.407254678436	139.977541281058, 354.221793586943	kg.m^2	Missile Iyy inertia vector
Autopilot.AirframeCharacteristics.IzzMissile	241.68610885491, 646.407254678436	139.977541281058, 354.221793586943	kg.m^2	Missile Izz inertia vector
Autopilot.OperationPoint.Altlist	0, 2000, 10000	0, 2000, 10000	m	Altitude points for gain lookup table
Autopilot.OperationPoint.Machlist	0.5, 0.8, 0.95, 1, 1.5, 3, 5.9	0.5, 0.8, 0.95, 1, 1.5, 3, 5.9	-	Mach points for gain lookup table
Autopilot.AutopilotParameters.Kroll2	[7 x 3 matrix]	[7 x 3 matrix]	-	Autopilot Gain
Autopilot.AutopilotParameters.Kroll1	[7 x 3 matrix]	[7 x 3 matrix]	-	Autopilot Gain
Autopilot.AutopilotParameters.Krpitch	[7 x 3 matrix]	[7 x 3 matrix]	-	Autopilot Gain
Autopilot.AutopilotParameters.Kipitch	[7 x 3 matrix]	[7 x 3 matrix]	-	Autopilot Gain
Autopilot.AutopilotParameters.Kppitch	[7 x 3 matrix]	[7 x 3 matrix]	-	Autopilot Gain
	[7 x 3 matrix]	[7 x 3 matrix]	-	Autopilot Gain
Autopilot.AutopilotParameters.Kiyaw	[7 x 3 matrix]	[7 x 3 matrix]	-	Autopilot Gain
Autopilot.AutopilotParameters.Kpyaw	[7 x 3 matrix]	[7 x 3 matrix]	-	Autopilot Gain

A.7 Aerodynamic Stability Margin

Variable	Baseline Value	Optimized Value	Units	Description
StaticStability.StaticStabilityMargin	0.80646	0.62717	caliber	Worst case static stability margin of the airframe
StaticStability.StaticStabilityGraph				String of a png figure
StaticStability.AirframeCharacteristics.MassMissile	119.7092862, 299.16682446	114.392300968539, 272.154893012669	kg	Missile mass vector
StaticStability.AirframeCharacteristics.XCgMissile	2.37690158037213, 3.29354326047954	1.90565028005158, 2.5546447105795	m	Missile center of gravity vector
StaticStability.AirframeCharacteristics.IxxMissile	1.40998421446312, 2.09697010311469	1.65921329853419, 2.3436601908172	kg.m^2	Missile Ixx inertia vector
StaticStability.AirframeCharacteristics.IyyMissile	241.68610885491, 646.407254678436	139.977541281058, 354.221793586943	kg.m^2	Missile Iyy inertia vector
StaticStability.AirframeCharacteristics.IzzMissile	241.68610885491, 646.407254678436	139.977541281058, 354.221793586943	kg.m^2	Missile Izz inertia vector

A.8 Structure First Mode Bending Frequency

Variable	Baseline Value	Optimized Value	Units	Description
BendingFrequency.YoungModulus	7.00E+10	7.00E+10	Nm^2	Young modulus of elasticity
BendingFrequency.TubeThickness	0.005	0.005	m	Tube thickness
BendingFrequency.TubeDiameter	0.175	0.1863	m	Tube mean diameter
BendingFrequency.MassMissile	119.7092862, 299.16682446	114.392300968539, 272.154893012669	kg	Missile mass vector
BendingFrequency.LengthMissile	6.5	5.04203	m	Missile length
BendingFrequency.FrequencyBending	105.90374185207, 66.991316096495	174.181061942788, 112.925301435039	rad/s	First Mode Bending Frequency of tube

A.9 Trajectory Computation

Variable	Baseline Value	Optimized Value	Units	Description
Trajectory.FighterPosEInit	0, 0, -5000	0, 0, -5000	m	The weapon position [x y z] at the beginning of simulation
Trajectory.FighterVelEInit	600, 0, 0	600, 0, 0	m/s	The weapon velocity [x y z] at the beginning of simulation
Trajectory.TargetPosEInit	100000, 0, 0	100000, 0, 0	m	The target position [x y z] at the beginning of simulation
Trajectory.TargetVelEInit	0, 0, 0	0, 0, 0	m/s	The target velocity [x y z] at the beginning of simulation
Trajectory.AirframeCharacteristics.MassMissile	119.7092862, 299.16682446	114.392300968539, 272.154893012669	kg	Missile mass vector
Trajectory.AirframeCharacteristics.XCgMissile	2.37690158037213, 3.29354326047954	1.90565028005158, 2.5546447105795	m	Missile center of gravity vector

Trajectory.AirframeCharacteristics.IxxMissile	1.40998421446312, 2.09697010311469	1.65921329853419, 2.3436601908172	kg.m^2	Missile Ixx inertia vector
Trajectory.AirframeCharacteristics.IyyMissile	241.68610885491, 646.407254678436	139.977541281058, 354.221793586943	kg.m^2	Missile Iyy inertia vector
Trajectory.AirframeCharacteristics.IzzMissile	241.68610885491, 646.407254678436	139.977541281058, 354.221793586943	kg.m^2	Missile Izz inertia vector
Trajectory.Motor.NozzleExitArea	0.02405	0.02726	m^2	Motor nozzle exit area
Trajectory.Motor.MotorMass	0, 0.001, 104.981164426571, 104.982164426571, 179.45653826, 179.45753826	0, 0.001, 36.7397345648084, 36.7407345648084, 157.76159204413, 157.76259204413	kg	thrust vs Rate MotorMassRemaining
Trajectory.Motor.ThrustSeaLevel	0, 4000, 4000, 35000, 35000, 0	0, 1271.17, 1271.17, 35000, 35000, 0	N	Thrust at sea level vector
Trajectory.Motor.SpecificImpulseMotor	219	219	s	Fuel Rate Spent
Trajectory.Trajectory.FlightTime	100.52	77.1753	s	Total Flight Time
Trajectory.Trajectory.MachOut	[Long vector]	[Long vector]	mach	Velocity Scalar
Trajectory.Trajectory.PoszE	[Long vector]	[Long vector]	m	Altitude
Trajectory.Trajectory.TimeOut	[Long vector]	[Long vector]	s	Time of simulation
Trajectory.TrajectoryShaping.WayPointTableX	0, 25000, 75000, 100000	0, 25000, 75000, 100000	m	Way Point Table X
Trajectory.TrajectoryShaping.WayPointTableY	0, 0, 0, 0	0, 0, 0, 0	m	Way Point Table Y
Trajectory.TrajectoryShaping.WayPointTableZ	0, -5000, -5000, 5000	0, -10000, -10000, 5000	m	Way Point Table Z
Trajectory.TrajectoryShaping.TrackingBandwith	1	1	rad/s	Tracking bandwith
Trajectory.TrajectoryShaping.MaxAcceleration	80	80	m/s^2	Max commanded acceleration
Trajectory.TrajectoryShaping.FilterTurnOnRange	4000	4000	m	Filter turn on range
Trajectory.AutopilotParameters.AltitudeList	0, 2000, 10000	0, 2000, 10000	m	Altitude points for gain lookup table
Trajectory.AutopilotParameters.MachList	0.5, 0.8, 0.95, 1, 1.5, 3, 5.9	0.5, 0.8, 0.95, 1, 1.5, 3, 5.9		Mach points for gain lookup table
Trajectory.AutopilotParameters.KpYaw	[7 x 3 matrix]	[7 x 3 matrix]	-	
Trajectory.AutopilotParameters.KiYaw	[7 x 3 matrix]	[7 x 3 matrix]	-	
Trajectory.AutopilotParameters.KrYaw	[7 x 3 matrix]	[7 x 3 matrix]	-	
Trajectory.AutopilotParameters.KpPitch	[7 x 3 matrix]	[7 x 3 matrix]	-	
Trajectory.AutopilotParameters.KiPitch	[7 x 3 matrix]	[7 x 3 matrix]	-	
Trajectory.AutopilotParameters.KrPitch	[7 x 3 matrix]	[7 x 3 matrix]	-	
Trajectory.AutopilotParameters.DeltaMax	0.2	0.2	rad	Maximum fin deflection
Trajectory.AutopilotParameters.Kroll1	[7 x 3 matrix]	[7 x 3 matrix]	-	
Trajectory.AutopilotParameters.Kroll2	[7 x 3 matrix]	[7 x 3 matrix]	-	

A.10 Aerodynamic Heating

Variable	Baseline Value	Optimized Value	Units	Description
Aeroheating.Interact.XGRID	0, 0.26743, 0.53486, 0.80229, 1.0697, 1.3371, 1.6046, 1.872, 2.1394, 2.4069, 2.6743, 2.9417, 3.2091, 3.4766, 3.744, 4.0114, 4.2789, 4.5463,	0, 0.19486, 0.38972, 0.58458, 0.77944, 0.9743, 1.1692, 1.364, 1.5589, 1.7537, 1.9486, 2.1435, 2.3383, 2.5332, 2.728, 2.9229, 3.1178, 3.3126,	caliber	GRID position in caliber

	4.8137, 5.0811, 5.3486, 5.5714, 5.8834, 6.1286, 6.4183, 6.6857	3.5075, 3.7023, 3.8972, 4.0596, 4.2869, 4.4655, 4.6766, 4.8715		
Aeroheating.Interact.QDOT	54601, -1138700, -805150, -657400, -569330, -509220, -464850, -430370, -402570, -379550, -360070, -343320, -328700, -315810, -304320, -294000, -284660, -276160, -268380, -261220, -254610, -249470, -241190, -236330, -230960, -226310	187790, -1222500, -864440, -705810, -611250, -546720, -499080, -462060, -432220, -407500, -386590, -368600, -352910, -339060, -326730, -315650, -305630, -296500, -288150, -280460, -273360, -267840, -250050, -245030, -239470, -234660	W/m^2	Heat transfer
Aeroheating.Interact.Geometry.XLE	0, 5.57142857142857, 6.12857142857143, 6.68571428571429	0, 4.05958132045089, 4.46553945249597, 4.87149758454106	caliber	X position of the body contour
Aeroheating.Interact.Geometry.R	0, 0.5, 0.5, 0.5	0, 0.5, 0.5, 0.5	caliber	Radius of the body contour at X position
Aeroheating.Interact.Geometry.DIAM	0.57415	0.61122	ft	Reference diameter
Aeroheating.Interact.Geometry.AREF	0.2589	0.29342	ft^2	Reference area
Aeroheating.Interact.Geometry.FLALEN	0.55714	0.40596	caliber	Flare length (caliber) (use 0 for no flare afterbody)
Aeroheating.Interact.Geometry.BETA	0	0	Deg	Flare angle (deg)
Aeroheating.Interact.Geometry.IFBLUNT	1	1	-	0 sharp nose body, 1 blunt node body
Aeroheating.Interact.Geometry.RCAP	0.22857	0.20353	caliber	Radius of nose cap (caliber) (used for ifblunt=1 only, otherwise set to 0)
Aeroheating.Interact.Geometry.NGRID	25	25		Number of streamwise grid points (odd integer)
Aeroheating.Interact.OperationPoint.Twall	5400	5400	^{o}R	Structure surface temperature in degrees Rankine
Aeroheating.Interact.OperationPoint.MINF	1.52439	2.44183	n/a	Freestream mach number
Aeroheating.Interact.OperationPoint.REYNUM	4.92E+06	1.01E+07	-	Reynolds number based on the total length of the body (uinf*length/viscosity)
Aeroheating.Interact.OperationPoint.PINF	1649.52	2115.44	lb/ft/ft	Freestream static pressure (lb/ft/ft)
Aeroheating.Interact.OperationPoint.RHOINF	0.00194	0.00238	slug/ft/ft/ft	Freestream density
Aeroheating.Interact.OperationPoint.AINF	1090.28	1116.39	ft/s	Freestream speed of sound (ft/s)
Aeroheating.Interact.OperationPoint.TINF	494.662	518.637	^{o}R	Freestream static temperature
Aeroheating.Interact.InteractParameters.XINTER	1	1	caliber	Beginning of anticipated interaction region
Aeroheating.Interact.InteractParameters.XTRANS	1	1	caliber	Location of boundary layer transition
Aeroheating.Interact.InteractParameters.ETAE	11.3	11.3		Eta at the edge of the boundary layer. Eta is the y-direction transformation variable defined as : eta = (y/l)*sqrt(reynum)*sqrt[(ue/uinf)/(x/l)].
Aeroheating.Interact.InteractParameters.INVOPT	5	5		Inviscid flow theory option :
Aeroheating.Interact.InteractParameters.NOPT	0	0		(Used for invopt=5,6 only) 0 modified-newtonian theory, 1 newton-busemann theory
Aeroheating.Interact.InteractParameters.GAMMAN	1.405	1.405		(Used for invopt=5,6 and nopt=1 only) value of gamma for newton-busemann theory

A.11 Conduction and Structure Temperature

Variable	Baseline Value	Optimized Value	Units	Description
Conduction.Tmax	2171.27	2188.54	K	Maximum temperature
Conduction.Geometry.XLE	0, 0.975, 1.0725, 1.17	0, 0.7563, 0.83193, 0.90756	m	X position of the structure contour
Conduction.Geometry.R	0, 0.0875, 0.0875, 0.0875	0, 0.09315, 0.09315, 0.09315	m	Radius of the structure contour at X position
Conduction.Geometry.RCAP	0.04	0.03792	m	Noze bluntness radius
Conduction.HeatTransfer.Q3000K	[100 x 26 matrix]	[100 x 26 matrix]	W/m^2	Heat Transfer for a 3000K surface temperature
Conduction.HeatTransfer.HTTime	[Long vector]	[Long vector]	s	Time vector
Conduction.HeatTransfer.Q300K	[100 x 26 matrix]	[100 x 26 matrix]	W/m^2	Heat Transfer for a 300K surface temperature
Conduction.HeatTransfer.XGRID	0, 0.26743, 0.53486, 0.80229, 1.0697, 1.3371, 1.6046, 1.872, 2.1394, 2.4069, 2.6743, 2.9417, 3.2091, 3.4766, 3.744, 4.0114, 4.2789, 4.5463, 4.8137, 5.0811, 5.3486, 5.5714, 5.8834, 6.1286, 6.4183, 6.6857	0, 0.19486, 0.38972, 0.58458, 0.77944, 0.9743, 1.1692, 1.364, 1.5589, 1.7537, 1.9486, 2.1435, 2.3383, 2.5332, 2.728, 2.9229, 3.1178, 3.3126, 3.5075, 3.7023, 3.8972, 4.0596, 4.2869, 4.4655, 4.6766, 4.8715	caliber	Station position along X axis for heat transfer
Conduction.Material.MaterialId	5	5	-	Material Al(1),St(2),W(3),SiC(4),C-C(5),C/P(6),G-E(7)
Conduction.Grid.Nx	20	20	-	Grid size in length
Conduction.Grid.Ny	5	5	-	Grid size in radius

List of acronyms

6DOF	Six-Degrees-Of-Freedom
CAD	Computer Aided-Design
CG	Center-Of-Gravity
DND	Department of National Defence
DRDC	Defence R&D Canada
GNC	Guidance, navigation and control
IHPS	Integrated Hypersonic Technologies For Long-Range Precision Strike
R&D	Research & Development
wrt	with respect to

This page intentionally left blank.

DOCUMENT CONTROL DATA

(Security classification of title, body of abstract and indexing annotation must be entered when the overall document is classified)

1. ORIGINATOR (The name and address of the organization preparing the document. Organizations for whom the document was prepared, e.g. Centre sponsoring a contractor's report, or tasking agency, are entered in section 8.)

Defence R&D Canada – Valcartier
2459 Pie-XI Blvd North
Quebec (Quebec)
G3J 1X5 Canada

2. SECURITY CLASSIFICATION (Overall security classification of the document including special warning terms if applicable.)

3. TITLE (The complete document title as indicated on the title page. Its classification should be indicated by the appropriate abbreviation (S, C, R or U) in parentheses after the title.)

Multidisciplinary integrated analysis for engagement simulation of hypersonic weapons

4. AUTHORS (last name, followed by initials – ranks, titles, etc. not to be used)

Richard Lestage; François Lesage; Robert A. Stowe, Nicolas Hamel

5. DATE OF PUBLICATION (Month and year of publication of document.)	6a. NO. OF PAGES (Total containing information, including Annexes, Appendices, etc.)	6b. NO. OF REFS (Total cited in document.)
May 2010	40	25

7. DESCRIPTIVE NOTES (The category of the document, e.g. technical report, technical note or memorandum. If appropriate, enter the type of report, e.g. interim, progress, summary, annual or final. Give the inclusive dates when a specific reporting period is covered.)

Technical Memorandum

8. SPONSORING ACTIVITY (The name of the department project office or laboratory sponsoring the research and development – include address.)

Defence R&D Canada – Valcartier
2459 Pie-XI Blvd North
Quebec (Quebec)
G3J 1X5 Canada

9a. PROJECT OR GRANT NO. (If appropriate, the applicable research and development project or grant number under which the document was written. Please specify whether project or grant.)	9b. CONTRACT NO. (If appropriate, the applicable number under which the document was written.)
13eu04	

10a. ORIGINATOR'S DOCUMENT NUMBER (The official document number by which the document is identified by the originating activity. This number must be unique to this document.)	10b. OTHER DOCUMENT NO(s). (Any other numbers which may be assigned this document either by the originator or by the sponsor.)
DRDC Valcartier TM 2010-085	

11. DOCUMENT AVAILABILITY (Any limitations on further dissemination of the document, other than those imposed by security classification.)

(X) Unlimited distribution
( ) Defence departments and defence contractors; further distribution only as approved
( ) Defence departments and Canadian defence contractors; further distribution only as approved
( ) Government departments and agencies; further distribution only as approved
( ) Defence departments; further distribution only as approved
( ) Other (please specify):

12. DOCUMENT ANNOUNCEMENT (Any limitation to the bibliographic announcement of this document. This will normally correspond to the Document Availability (11). However, where further distribution (beyond the audience specified in (11) is possible, a wider announcement audience may be selected.))

Unlimited

13. ABSTRACT (A brief and factual summary of the document. It may also appear elsewhere in the body of the document itself. It is highly desirable that the abstract of classified documents be unclassified. Each paragraph of the abstract shall begin with an indication of the security classification of the information in the paragraph (unless the document itself is unclassified) represented as (S), (C), (R), or (U). It is not necessary to include here abstracts in both official languages unless the text is bilingual.)

The emergence of missiles flying in the hypersonic regime brings a new series of technical challenges such as, strong system integration of aerodynamics, propulsion and structures, and problems with thermal management. To address these challenges, a multidisciplinary integrated analysis tool which permits to perform a complete engagement simulation using a six-degree-of-freedom flight mechanics models was developed. The tool is used to perform parametric study for missile sizing, performance trade-off and optimization. Additionally, it assesses the effect of vehicle design variables on the flight time, the trajectory and the velocity profile. A baseline missile reference was established as a starting point on which the impact of various design variables is assessed. The various sensitivity and trade-off analyses performed on key missile design variables allowed observing several interesting interactions and learning key lessons to apply to the design and analysis of hypersonic missiles. To demonstrate the application of optimization techniques to the design of hypersonic missiles, a simple time of flight optimization problem is presented. The multidisciplinary integrated analysis tool presents basic analysis capabilities for all subsystems critical to the study of hypersonic weapon systems. However, most subsystem models are limited in fidelity and details and would benefit from improvements. The most significant deficiencies are the lack of an airbreathing propulsion model and the non support of non-symmetric airframe configurations such as wave-riders. The support of wave-rider type configurations would require significant changes to most subsystems models.

14. KEYWORDS, DESCRIPTORS or IDENTIFIERS (Technically meaningful terms or short phrases that characterize a document and could be helpful in cataloguing the document. They should be selected so that no security classification is required. Identifiers, such as equipment model designation, trade name, military project code name, geographic location may also be included. If possible keywords should be selected from a published thesaurus, e.g. Thesaurus of Engineering and Scientific Terms (TEST) and that thesaurus identified. If it is not possible to select indexing terms which are Unclassified, the classification of each should be indicated as with the title.)

Missile, Optimization, hypersonic, multidisciplinary analysis, design trade-off

Defence R&D Canada

Canada's Leader in Defence
and National Security
Science and Technology

R & D pour la défense Canada

Chef de file au Canada en matière
de science et de technologie pour
la défense et la sécurité nationale

DEFENCE R&D DÉFENSE

www.drdc-rddc.gc.ca